Optimizing AI Reasoning: A Hamiltonian Dynamics Approach to Multi-Hop Question Answering

Javier Marín (javier@jmarin.info)

October 5, 2024

ABSTRACT

This paper introduces an innovative approach to analyzing and improving multi-hop reasoning in AI systems by drawing inspiration from Hamiltonian mechanics. We propose a novel framework that maps reasoning chains in embedding spaces to Hamiltonian systems, allowing us to leverage powerful analytical tools from classical physics. Our method defines a Hamiltonian function that balances the progression of reasoning (kinetic energy) against the relevance to the question at hand (potential energy). Using this framework, we analyze a large dataset of reasoning chains from a multi-hop question-answering task, revealing intriguing patterns that distinguish valid from invalid reasoning. We show that valid reasoning chains have lower Hamiltonian energy and move in ways that make the best trade-off between getting more information and answering the right question. Furthermore, we demonstrate the application of this framework to steer the creation of more efficient reasoning algorithms within AI systems. Our results not only provide new insights into the nature of valid reasoning but also open up exciting possibilities for physics-inspired approaches to understanding and improving artificial intelligence.

Keywords: Natural Language Processing, Multi-hop Reasoning, Hamiltonian Mechanics, Explainable AI, Cognitive Computing

1. Introduction

1.1. Motivation for a physics-inspired approach

The scientific method, integrating mathematical abstractions and empirical observation, has been essential for furthering our understanding of the universe and its underlying laws (Popper, 1959) The progression of scientific thought illustrates how human mind has systematically deciphered the complexity of the world, resulting in notable technical achievements (Kuhn, 1962). Formal representations, especially mathematical equations, function as effective instruments for encoding physical processes (Wigner, 1990). These abstract constructs have distinct rules and exist in a conceptual domain that can be accessed, manipulated, and comprehended by the human intellect(Penrose, 2006). This method entails generating predictions regarding the physical world derived from theoretical models, which are then validated by experimentation.

This approach's philosophical framework includes ontological considerations about the existence of abstract objects beyond physical reality (Quine, 1948), epistemological questions into how the human mind acquires knowledge of this abstract domain (Goldman, 1967), and the concept of structural realism, which asserts that structures in the abstract realm correspond to those in the physical world (Worrall, 1989). The concept of universal structural realism proposes that the physical universe is isomorphic to a mathematical structure (Tegmark, 2008). The notable success of physics in formulate complex phenomena using advanced mathematical frameworks suggests that similar approaches may be effectively utilized in other fields, such as AI and cognitive science (Carleo et al., 2019). In physics, formal representations like equations and models function as powerful instruments for describing and predicting physical phenomena (Feynman, 1967). These abstractions facilitate the encoding of essential elements of complex systems in a way that is suitable to manipulation, assessment, and practical application (Andersen, 1972). The successes of physics-based methodologies in various scientific fields (Barabási & Albert, 1999; Bialek, 2012) provide a strong justification for exploring their relevance in AI, especially regarding the assessment and improvement of models' reasoning capabilities (Carleo et al., 2019; Mehta et al., 2019). Similar to how physicists apply mathematical models to explain the behavior of elementary particles, quantum fields, and particle states (Weinberg, 1995), we propose the use of analogous formalisms for

describing the dynamics of reasoning within embedding spaces (Bengio et al., 2013; Mikolov et al., 2013a) .

This physics-based methodology provides a robust framework for examining the intricate cognitive processes associated with AI reasoning, potentially yielding innovative discoveries and advancements in the discipline (Wu et al., 2020). If I had to summarize it explicitly I would include the following points: The efficiency of embedding methods for conveying semantic information in AI systems closely parallels the application of abstract spaces in physics, such as phase space in classical mechanics or Hilbert space in quantum mechanics.The reasoning process in Question-Answering, QA, advancing from premises to conclusions, resembles the development of physical systems governed by fundamental laws like symmetries, conservation laws and Hamiltonian mechanics. The need for measurable and objective assessments of multi-hop QA systems could benefit from the rigorous, mathematically-based methods for evaluating in physics.

1.2.   Background on multi-hop reasoning in AI

Multi-hop question-answering, where multiple facts are needed to derive an answer, is an important step to perform complex reasoning and provide explanations for answers in Language Models, LMs (Yang et al., 2018a). QA provides a quantifiable and objective way to test the reasoning ability of intelligent systems. QA tasks provide numerical metrics such as accuracy, F1 score, or mean reciprocal rank, allowing for precise comparison between different AI systems. QA assignments generally have clearly defined correct answers, hence reducing subjectivity in evaluation and minimizing human bias in assessment. QA function can be designed to evaluate several facets of reasoning, including deductive reasoning or deriving conclusions from established premises, inductive reasoning or generalizing from particular instances, and abductive reasoning or formulating the most plausible answer from partial knowledge (Garbuio & Lin, 2021).

Recent developments using knowledge graphs struggle to model multi-hop relations efficiently, or lack transparency into the model's prediction rationale (Feng et al., 2020). Knowledge graphs (KGs) neglect the latent relational information among question concepts and answers. (Dong et al., 2023) suggested a hierarchy-aware methodology that uses hierarchical structures in knowledge graphs to enhance comprehension and reasoning about complex questions, addressing the flaw of prior approaches that mostly emphasized language models for context encoding. This method captures more complex interconnections between concepts and facilitates a thorough understanding of semantic connections that may remain hidden in simpler representations. Hierarchical architectures facilitate advanced reasoning patterns that mimic human cognitive processes. It can more successfully address challenging questions requiring multi-step or multi-level reasoning (Wang et al., 2022).

We have several challenges to improve reasoning processes. One of the most important requirements is the interpretability and explainability of models (Singh et al., 2024). The difficulty in understanding the internal reasoning process of complex AI models, especially deep neural networks, limits their real assessment and the capability of generating human-understandable explanations for AI decisions and inferences (Lipton, 2018; Ribeiro et al., 2016). Ensuring that reasoning processes are robust to slight variations in input or context, and developing models that can generalize reasoning skills across different domains and types of questions is another key target we must address to improve the reasoning process (Bengio et al., 2021; Geirhos et al., 2020). Without these efforts, we are struggling in identifying and mitigating biases in reasoning processes, ensuring fair reasoning across different demographic groups or topic areas (Mehrabi et al., 2021). We have also some challenges in scaling up reasoning capabilities to handle increasingly complex and multi-step problems and integrating updated external knowledge (Bender et al., 2021). It is important to enhance thinking processes that can tackle partial or uncertain information. (Jhamtani & Clark, 2020a; Singh et al., 2024). Addressing ambiguity in natural language questions and contexts will be decisive for improving the model's reasoning abilities, as will the development of new metrics that overcome existing ones' limits in capturing the nuances of complex reasoning. In seeking to develop autonomous co-workers using LLMs, we must confront the problems of temporal and causal thinking, particularly in the modeling and analysis of temporal sequences and causal relationships (Maruthi et al., 2022). Additional issues like ethical reasoning, adversarial attacks (Zhang et al., 2020), long-term consistency, and human-AI collaboration (Järvelä et al., 2023) will require substantial revision to develop really reasoning models.

An further important roadblock in enhancing the model's reasoning process are the training datasets. Recent multi-hop question answering datasets seek to address several shortcomings of earlier multi-hop QA datasets (Ho et al., 2020; Jhamtani & Clark, 2020b; Welbl et al., 2018; Yang et al., 2018b). These new datasets provide thorough elucidations of the reasoning process from QA, rectifying deficiencies in existing datasets. They additionally provide "evidence information", which defines a reasoning pathway for multi-hop inquiries, supplying comprehensive explanations for predictions and simplifying the evaluation of a model's reasoning abilities (Dua et al., 2019; Khot et al., 2020). Moreover, these datasets address the issue noted in earlier proposals, where several examples lacked the necessity for multi-hop reasoning, by using logical rules to generate questions that are both natural and require multi-hop reasoning (Chen & Durrett, 2019). The mechanisms for generating question-answer pairs aim to guarantee both the multi-hop processes and the quality of the questions. These datasets may improve the development of more transparent AI systems in question answering and create a new, possibly

rigorous standard for evaluating and developing multi-hop QA systems.

2. Hamiltonian of dynamical systems

2.1. Brief review of Hamiltonian mechanics

The Hamiltonian formalism provides an effective mathematical framework for developing conservative mechanical system theory and is a geometric language for multiple fields of physics. A Hamiltonian can be defined with the following $2n$ ordinary differential equations (Easton, 1993):

$$\dot{q} = H_p \, , \qquad \dot{p} = -H_q \qquad (1)$$

$$\dot{q}_l = \frac{\partial H}{\partial p_l}(t, q, p) \, , \qquad p_i = -\frac{\partial H}{\partial q_i}(t, p, q) \qquad (2)$$

where $H = H(t, q, p)$ is the Hamiltonian, q and p are the position and momentum vectors of a mechanical system with n degrees of freedom, and t is the time. In these equations $(t, q, p) \in \mathcal{O}$ – an open set in $\mathbb{R}^1 \times \mathbb{R}^n \times \mathbb{R}^n, and \ 1 < i < n$. Given the Lagrangian (De León & Rodrigues, 2011)

$$L = T - U \qquad (3)$$

where T is the kinetic energy and U is the potential energy. We can rewrite this equation as

$$L = T(q, \dot{q}) - U(q) \qquad (4)$$

$$\frac{d}{dt}\left(\frac{\partial L}{\partial \dot{q}}\right) = \frac{\partial L}{\partial q} \qquad (5)$$

This is the Euler-Lagrange equation describing the motions of the system, and is equivalent to the Hamiltonian system (Hairer et al., 2006):

$$H(q, p, t) = p^T \dot{q} - L(q, \dot{q}, t) \qquad (6)$$

Hamiltonian equations can be rewritten as

$$\dot{q} = \nabla_p H(q, p), \qquad \dot{p} = -\nabla_q H(q, p) \qquad (7)$$

The Hamiltonian formalism introduces the concept of phase space, a $2n$-dimensional space where n is the number of degrees of freedom. Each point in phase space represents a unique state of the system, defined by its position and momentum coordinates (q, p). The phase space of a Hamiltonian system is a symplectic manifold, and Hamiltonian flows preserve the symplectic structure (Goldman, 1984). Symplectic structures are fundamental geometric objects in differential geometry and classical mechanics (Goldman, 1984). This objects provide a

framework for understanding the relationship between position and momentum in physical systems, allowing for the formulation of Hamilton's equations of motion. Simply said, symplectic structures are specific rules that define how things move in physics, similar to an equation for motion. They help us grasp how items' positions and velocities are related, allowing us to predict how things will behave over time.

Formally, a symplectic structure on a smooth manifold M is a closed, non-degenerate 2-form ω. This structure on an even-dimensional manifold M satisfies two key properties (Goldman, 1984):

a) Closure: $d\omega = 0$, where d is the exterior derivative.
b) Non-degeneracy: For each point p in M, the map $v \mapsto \omega_p(v, \cdot)$ from the tangent space $T_p M$ to its dual is an isomorphism (Goldman, 1984).

These structures allow for the definition of Poisson brackets and canonical transformations (Easton, 1993). In local coordinates (q_i, p_i), a standard symplectic form can be written as $\omega = \sum_i dq_i \wedge dp_i$. According Liouville's theorem, these structures preserve phase space volume (Prugovečki, 1979). They ensure the conservation of certain geometric properties under the flow of Hamiltonian vector fields. Symplectic structures and Poisson brackets (section 2.2) are fundamental tools from classical mechanics that we adapt to analyze reasoning processes in AI systems. By mapping reasoning chains to trajectories in a symplectic space, we can use these concepts to quantify the "energy" and dynamics of cognitive processes, potentially umveiling underlying principles of effective reasoning and guiding the development of more robust AI algorithms.

2.2. The Poisson bracket

A key feature of Hamiltonian systems is the conservation of energy. In isolated systems, the Hamiltonian system $H(q, p, t)$ remains constant over time, representing the "total energy" of the system

$$\frac{dH}{dt} = \frac{\partial H}{\partial t} + \{H, H\} = \frac{\partial H}{\partial t} = 0 \qquad (8)$$

where $\{,\}$ denotes the Poisson bracket operator (Karasev & Maslov, 2012). Many of the special properties of Hamiltonian systems are formulated in terms of the Poisson bracket operator. Let H, F, and G be smooth functions from an open set $\mathcal{O}$ in $\mathbb{R}^1 \times \mathbb{R}^n \times \mathbb{R}^n$, the Poisson bracket of F and G is defined as (Easton, 1993) :

$$\{F, G\} = \nabla F^T J \nabla G = \frac{\partial F^T}{\partial q} \frac{\partial G}{\partial p} - \frac{\partial F^T}{\partial p} \frac{\partial G}{\partial p} \qquad (9)$$

where $\{F, G\}$ is a smooth map from $\mathcal{O}$ to $\mathbb{R}^1$. We can verify that $\{\cdot, \cdot\}$ is skew-symmetric and bilinear When H is independent

of t, a critical point of H as a function represents an equilibrium point of the Hamiltonian system's differential equations.

2.3. Canonical transformations

Canonical transformations are an essential component in Hamiltonian mechanics. Generalized canonical transformations for generalized Hamiltonian systems transform one Hamiltonian system into another while maintaining the original structure (Fujimoto & Sugie, 2001). Similar to classical mechanics, canonical transformations are expected to provide new insights and fundamental tools for the analysis these systems. A set of transformations of x, y and H, we say that is a canonical transformation for generalized Hamiltonian systems if it transforms the time-varying generalized Hamiltonian system into another one (Fujimoto & Sugie, 2001).

$$\bar{x} = \Phi(x, t) \qquad (10.1)$$

$$\bar{H} = H(x, t) + U(x, t) \qquad (10.2)$$

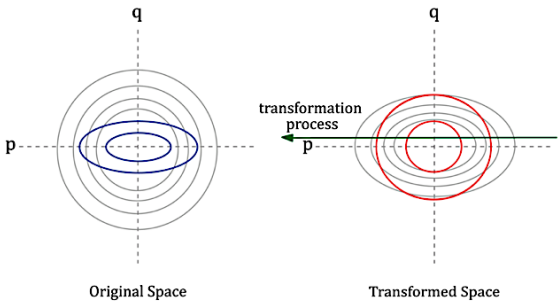$$\bar{y} = y + \alpha(x, t) \qquad (10.3)$$

Figure 1: Canonical Transformations in Reasoning Space

Figure 1 illustrates the basic idea of canonical transformations used in our Hamiltonian model. The composition has two phase plots: the "Original Space" on the left and the "Transformed Space" on the right. The original space denotes the initial model. Elliptical trajectories indicate fluctuating rates of change in states and momentum, while contour lines denote energy levels. The transformed framework exhibits the identical system subsequent to the implementation of a canonical transformation. Circular trajectories indicate a more consistent advancement across states. Modified contour lines indicate a revised energy distribution. $\Phi(x, t)$ correlates original reasoning states with new ones. $H(x, t) + U(x, t)$ modifies the Hamiltonian (total energy) by incorporating an additional term $U(x, t)$. Finally, $y + \alpha(x, t)$ transforms the momentum. The green arrow in the illustration indicates the operation of the canonical transformation. The arrow represents the transformation process from the left plot (Original Space) to the right plot (Transformed Space). It reflects the mapping of locations, trajectories, and energy

levels from the original space to their corresponding elements in the transformed space. The arrow's smoothness indicates that the transformation is continuous and clearly specified for all points within the reasoning space.

3. A new framework for reasoning systems

3.1. Hamiltonian framework for reasoning

3.1.1. Defining the reasoning state space

In our analogy, we can represent reasoning states as vectors in a high-dimensional embedding space (Mikolov et al., 2013b). This embedding space is derived from a pre-trained language model (Devlin, 2018), capturing the semantic content of each reasoning step. Formally, we define the reasoning state q as:

$$q = E(x) \in \mathbb{R}^d \qquad (11)$$

where $E: V \rightarrow \mathbb{R}^d$ is the embedding function, V is the vocabulary of the language model, and $x \in V^*$ is the input text (e.g., a fact or question in the reasoning chain). The input text x is first tokenized into a sequence of tokens $(t_1, t_2, \ldots, t_n)$ using the LLM's tokenizer T. Each token t_i is mapped to its corresponding embedding vector e_i:

$$e_i = E_{token}(t_i) \in \mathbb{R}^d \qquad (12)$$

The model then processes these token embeddings (Sennrich, 2015) through its layers (e.g., transformer layers) to produce contextual embeddings:

$$(c_1, c_2, \ldots, c_n) = model([e_1, e_2, \ldots, e_n]) \qquad (13)$$

where $c_i \in \mathbb{R}^d$ are the contextual embeddings. Finally, we aggregate these contextual embeddings to represent the entire input:

$$q = A(e_1, e_2, \ldots, c_n) \qquad (14)$$

where A is an aggregation function (Reimers, 2019), which could be mean pooling,

$$q = \left(\frac{1}{n}\right) \sum_i c_i \qquad (15)$$

max pooling, $q_j = max_i(c_i)_j$ for each dimension j, or $[CLS]\ token: q = c_1$ (assuming the first token is a special [CLS] token).

3.1.2. Hamiltonian for reasoning chains

A reasoning chain can be represented as a sequence of states $Q = (q_1, q_2, \ldots, q_m)$ where each $q_i \in \mathbb{R}^d$. We define a Hamiltonian for reasoning $H_R: \mathbb{R}^d \times \mathbb{R}^d \to \mathbb{R}$ as:

$$H_R(q, p) = T(p) - V(q) \qquad (16)$$

where q represents the current state of reasoning, analogous to position in mechanical systems, and p represents the change in reasoning, analogous to momentum (Friston, 2010). The reasoning momentum p can be defined as the difference between consecutive states $p_i = q_{\{i+1\}} - q_i$. $T(p)$ is the "kinetic" term representing the cost of changing the reasoning state, and $V(q)$ is the "potential" term representing the relevance or correctness of the current reasoning state. The notation R denotes that is a reasoning system. Note that this equation is similar to Lagrangian equation already introduced. Although Lagrangian mechanics is contained in Hamiltonian mechanics as a special case, "the Hamiltonian point of view allows us to solve completely a series of mechanical problems which do not yield solutions by other means" (Glattfelder, 2019). The kinetic term $T(p)$ can be interpreted as the cognitive effort or computational cost associated with changing the reasoning state (Friston, 2010). We define this effort as:

$$T(p) = \frac{1}{2}\|p\|^2 \qquad (17)$$

where $\|p\|$ is the magnitude of the change vector. This quadratic form is analogous to kinetic energy in classical physics and penalizes large, rapid changes in reasoning. The term $V(q)$ represents the degree to which the present reasoning state corresponds with the objective or question being addressed. A lower potential energy indicates a more relevant or realistic state. We could define it as:

$$V(q) = -sim(q, q_d) \qquad (18)$$

where $sim(\,,)$ is a similarity function like cosine similarity (Rahutomo et al., 2012), and q_d is the embedding of the desired answer or goal state.

$$sim(\vec{q}, \overrightarrow{q_d}) = \frac{\vec{q} \cdot \overrightarrow{q_d}}{\|\vec{q}\| \, \|\overrightarrow{q_d}\|} \qquad (19)$$

$\vec{q}$ and $\overrightarrow{q_d}$ are represented as two non-zero vectors in an inner product space. The reasoning phase space (q, p) inherits the symplectic structure discussed earlier. This implies that our reasoning Hamiltonian will preserve certain geometric properties as it evolves, analogous to the conservation of phase space volume in dynamical systems (Strogatz, 2018). We can apply canonical transformations to our reasoning Hamiltonian $H_R(q, p)$, allowing us to change variables while preserving the fundamental structure of the system (Arnold & Igorevich, 2013). We can write this transformation as:

$$\bar{x} = \Phi(x, t) \qquad (20.1)$$

$$\overline{H_R} = H_R(x, t) + U(x, t) \qquad (20.2)$$

$$\bar{y} = y + \alpha(x, t) \qquad (20.3)$$

where x represents our original phase space variables (q, p), and $(\bar{x}, \bar{y})$ represents the transformed variables. $\overline{H_R}$ is the transformed Hamiltonian, and $U(x, t)$ is a generating function for the transformation.

A special case in Hamiltonian systems is when we represent them in a 2D space ($H_R: \mathbb{R}^2 \times \mathbb{R}^2 \to \mathbb{R}$). The importance of recognizing a system as Hamiltonian lies in the ability to build the phase view without requiring a solution to the system (Hirsch et al., 2013). Assuming that H is not constant on any open set, we proceed with drawing the level curves $H(q, p) = constant$. The solutions of the system lie on these level sets; our objective is to determine the orientations of the solution trajectories on these level sets. This is straightforward due to the presence of the vector field. It is important to note that the equilibrium points of a Hamiltonian system are located at the critical points of H, namely at the places where both partial derivatives of H equal zero.
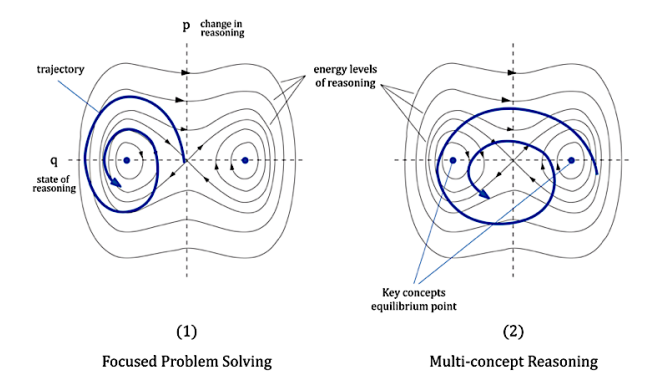

Figure 2: Phase plots for focused and multi-concept reasoning in a 2D Hamiltonian system

Figure 2 illustrates a phase plot for a reasoning system, with the q-axis denoting the current state of reasoning, similar to position in mechanical systems, and the p-axis indicating the change in reasoning, analogous to momentum. The contour lines denote the energy levels associated with reasoning. The blue lines illustrate potential reasoning paths and the evolution of reasoning over time within the phase space. The blue dots indicate stable states or key concepts. Figure 2.1 illustrates a focused problem-solving approach, characterized by tighter orbits around a singular concept, reflecting a concentrated emphasis on a single concept. Figure 2.2 illustrates a multi-concept reasoning framework, illustrating a larger orbit that includes several key concepts, thereby representing the integration of multiple reasoning levels.

In the context of our reasoning system, these transformations allow us to change the representation of our reasoning state while preserving the fundamental structure of the system. It also introduces new variables that may provide insights into

the reasoning process, simplifying the analysis of the reasoning dynamics by choosing appropriate transformations. For example, we can use a transformation to move from a word embedding space to a more abstract concept space, or to focus on particular aspects of the reasoning process. The ability to perform these transformations, while maintaining the canonical structure of our Hamiltonian is key to the flexibility and capability of this approach. It allows us to analyze the reasoning process from multiple perspectives and at different levels of abstraction, all within the same theoretical framework. The geometry of this embedding space is essential for understanding reasoning dynamics (Pennington et al., 2014) and will be presented in section 3.2.

3.1.3. Calculation of Hamiltonian energies for reasoning

We assume an optimal reasoning process in which the total energy H_R remains invariant. This implies a trade-off between exploration (high T, low V) and exploitation (low T, high V) during the reasoning process. This trade-off is analogous to key principles in reinforcement learning and statistical physics. In RL, it proves as the balance between trying new actions (exploration) and leveraging known good strategies (exploitation) (Kaelbling et al., 1996). In physical systems, it appears in phenomena like simulated annealing (Bertsimas & Tsitsiklis, 1993), where high temperatures allow broad exploration of state space, while low temperatures exploit known low-energy configurations. Our Hamiltonian formulation provides a rigorous mathematical framework for analyzing this trade-off in reasoning processes, potentially leading to new insights into optimal reasoning strategies and their connections to learning and physical systems. A practical application of this this trade-off in reasoning processes would be to explicitly define $T(p)$ and $V(q)$ in terms of exploration and exploitation measures in our reasoning space. Then we can analyze how different reasoning strategies balance T and V over time to find successful reasoning chains exhibiting a particular T/V ratio or evolution pattern. We can explore associations with RL algorithms, potentially adapting approaches such as Thompson sampling (Russo et al., 2018), or intrinsic motivation (Barto, 2013), to guide reasoning processes. It will be very stimulating to consider quantum analogies, where "superposition" could represent simultaneous exploration of multiple reasoning paths (Elsage et al., 2022).

To calculate the Hamiltonian energies for each reasoning chain, we follow these steps:

a) Embed each fact and question in the reasoning chain using the embedding function E.
b) Calculate $p = q_{t+1} - q_t$ as the difference between consecutive reasoning states.
c) Compute $T(p)$ and $V(q)$.
d) Calculate the total Hamiltonian energy H_R.

We perform these calculations for each step in the reasoning chain, allowing us to analyze the energy profile of the complete reasoning process.

3.2. Geometric analysis of reasoning trajectories

The application of differential geometry to reasoning trajectories offers a robust framework for studying the structure and attributes of cognitive processes. By conceptualizing reasoning paths as curves within a high-dimensional space, we can apply mathematical tools from differential geometry to measure and describe the properties of these paths (Amari, 2016). This approach allows us to move beyond simple distance metrics in embedding spaces and consider the intrinsic geometry of reasoning trajectories.

3.2.1. Differential geometry in cognitive spaces

In our framework, we consider reasoning processes as paths $\gamma(t)$ in a high-dimensional manifold M, which represents the space of possible cognitive states. This manifold is equipped with a metric g, which defines distances and angles in the cognitive space (Do Carmo, 2016). The metric captures the semantic similarity between different cognitive states and can be derived from embedding models such as BERT or GPT (Devlin, 2018). The tangent vector $\gamma'(t)$ at each point represents the instantaneous direction and speed of reasoning, while higher-order derivatives capture how this direction changes over time. This geometric perspective allows us to analyze both the content and the dynamics of reasoning processes.

3.2.2. Trajectories' curvature and cognitive flexibility

One of the key geometric properties we can analyze is the curvature of reasoning trajectories. For a curve $\gamma(t)$, the curvature κ at a point is given by:

$$\kappa = \frac{|\gamma''(t) \times \gamma'(t)|}{|\gamma'(t)|^3} \qquad (21)$$

where $\times$ denotes the cross product and $|\cdot|$ the magnitude (O'neill, 2006). In the context of reasoning, curvature can be interpreted as a measure of "cognitive flexibility" or the rate at which the direction of reasoning chain changes. High curvature indicates rapid shifts in reasoning direction, potentially representing moments of insight or the integration of diverse ideas. Low curvature suggests more linear, focused reasoning (Sussillo & Barak, 2013).

3.2.3. Frenet-Serret framework and multi-aspect reasoning

The Frenet-Serret theorems provide mathematical measurements for turning and twisting a curve in $\mathbb{R}^3$. Let

$\beta: I \longrightarrow \mathbb{R}^3$ be a unit speed curve with curvature $\kappa > 0$ and torsion τ (O'neill, 2006)

$$T'(t) = \kappa(t)N(t) \qquad (22.1)$$

$$N'(t) = -\kappa(t)T(t) + \tau(t)B(t) \qquad (22.2)$$

$$B'(t) = -\tau(t)N(t) \qquad (22.3)$$

T, N, and B are the tangent, normal, and binormal unit vectors. $T = \beta'$ is the unit tangent vector field of β, and has a constant length of 1. Then its derivative $T' = \beta''$ measures how the curve is turning. N is the principal vector field of β, and $B = T \times N$ is the binormal vector field of β (figure 3.1).

(1)   (2)
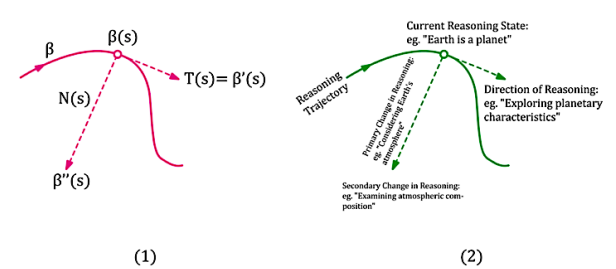
Figure 3. Representation of curvature with Frenet frame field.

In our framework, T represents the current direction of reasoning, N indicates the primary direction of change in reasoning, B captures secondary changes orthogonal to both T and N, and τ quantifies how the osculating plane (spanned by T and N) changes along the curve (Figure 3). This framework allows us to analyze not just the "bendiness" of a reasoning path, but also how it twists in the high-dimensional concept space, providing insights into multi-aspect reasoning processes.

Figure 3.1 illustrates the progression of a reasoning chain from an initial point, altering its trajectory as new elements are evaluated, potentially diverging into secondary issues, all while preserving the geometric connections defined by the Frenet-Serret framework. The Frenet frame field offers a more natural method to visualize and understand complex reasoning processes in AI systems. High curvature or torsion points in reasoning processes may represent critical choice points or insights, facilitating targeted interventions or optimizations. Different reasoning processes may be geometrically contrasted, thereby facilitating the identification of more efficient or successful methods. Consider a large e-commerce company deploying an AI-driven customer attention chatbot. With the this framework to examine the chatbot's reasoning processes, the organization could characterize client interactions, with each interaction represented as a curve within the reasoning space (Figure 4). We can get insights about the current direction of reasoning, $T(s)$, identify shifts in topic during conversation, $N(s)$, or unforeseen developments in conversation, $B(s)$. The curvature, κ, would show the rate at which the discussion is altering direction, while the torsion, τ, would indicate the

conversational framework is evolving (Figure 4). Geometric analysis would allow to find optimal trajectories (minimal curvature) for frequent inquiries from customers, and identifying situations when high curvature is needed, for example in difficult problems requiring substantial changes in strategy.
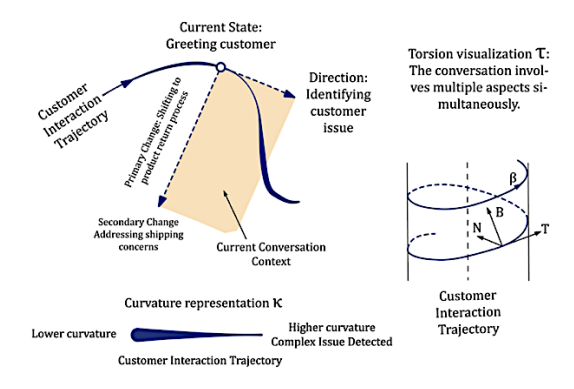

Figure 4. Representation of curvature for a large e-commerce company chatbot example.

Torsion analysis can be used to prepare the chatbot for complex, multi-concept challenges (Figure 2). In summary Frenet frame would allow us to assess successful contacts (those resulting in resolution and elevated customer satisfaction) to discern ideal geometric patterns and use them to prepare the chatbot to observe these patterns, modifying its strategy according on real-time geometric analysis of the dialogue.

3.2.4. Arbitrary speed curves

Given a regular curve $\beta: I \rightarrow \mathbb{R}^3$ with speed function v, we can calculate its velocity and acceleration (O'neill, 2006) as:

$$\beta' = vT \qquad (23.1)$$
$$\beta'' = \frac{dv}{dx}T + \kappa v^2 N \qquad (23.2)$$

where T is the tangent to the curve, and κ is the curvature in Frenet frame. This equation has two parts: $\frac{dv}{dx}T$ is a tangential component and measures the rate of change of β', and $\kappa v^2 N$ is the normal that points perpendicular to motion. The normal is a vector that represents a force acting at a 90-degree angle to the axis of motion, which does not alter the object's velocity in the direction of its original motion. According to Newton's laws of motion, this normal will create an angle such that a part of its velocity is now aligned with the normal direction. The two components combine to generate diagonal velocity at an angle dependent upon the magnitude of the applied force.
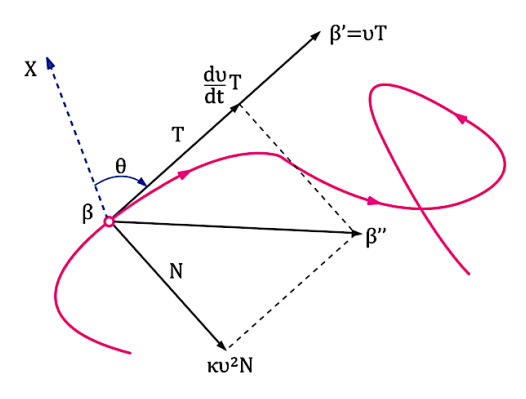
Figure 5. Velocity, acceleration and trajectory angle in a curve using Frenet frame.

In the context of reasoning, the velocity of reasoning advancement defines a "magnitude". A higher magnitude implies swifter transitions between ideas or ideas, whereas a smaller magnitude denotes a more gradual progression. This magnitude likewise represents the ″distance″ between successive concepts in reasoning. Large magnitude values exhibit substantial leaps between divergent ideas, whereas small magnitude values show progressive progress between closely related ideas. Acceleration in reasoning represents the changes in velocity over time. An increase in acceleration suggests an intense rate of ideation or problem-solving, while a decrease in acceleration indicates a deliberate deceleration to concentrate on particular elements.

In the Frenet frame, the trajectory angle can be interpreted as the angle between the tangent vector T and a fixed reference direction (Figure 5). This angle changes as the curve evolves, reflecting changes in the direction of reasoning. The rate of change of this angle is directly related to the curvature κ. The term $\kappa v^2 N$ represents the normal component of acceleration, which is responsible for changing the direction of velocity. We can define the trajectory angle θ as

$$\frac{d\theta}{dt} = \kappa v \quad (24)$$

This equation correlates the angular rate of change with the trajectory′s curvature and velocity or magnitude. A high magnitude might indicate creative, divergent thinking processes (Beaty et al., 2018), while decreasing magnitude over time could represent a convergence towards a solution or conclusion (Zabelina & Andrews-Hanna, 2016). Sudden large magnitude transitions might correspond to moments of insight or breakthrough in problem-solving (Kounios & Beeman, 2014a), while consistent, moderate magnitude transitions could indicate systematic, analytical thinking (Hélie & Sun, 2010). Understanding these dynamics can help in analyzing and potentially optimizing reasoning processes in both human cognition and AI systems. An AI system designed for creative work may be optimized for rapid transitions, whereas one built for analytical tasks can be tuned for steady, measured progressions. Cognitive processes can be viewed as

continuous trajectories in state spaces (Spivey & Dale, 2006). The trajectory angle θ might represent the current direction of reasoning in the conceptual space. Changes in θ indicate shifts in the focus or approach of the reasoning process. For example rapid changes in θ might correspond to creative leaps or sudden insights (Beaty et al., 2014), and slow, steady changes in θ could represent methodical, analytical reasoning (Kounios & Beeman, 2014b). Magnitude indicates the rate at which an AI system advances through various concepts, whereas θ denotes the trajectory. In combination, they offer a more comprehensive understanding of the trajectory of reasoning.

3.3. Symmetry and conservation laws in reasoning processes

The Hamiltonian framework developed in this paper provides a powerful lens through which to view and understand conservation laws in physical systems, particularly in the context of reasoning processes. This connection between symmetry and conservation, first formalized by Emmy Noether in 1918 (Kosmann-Schwarzbach et al., 2011), reveals deep insights into the nature of invariance in physical and cognitive systems. Our analysis of reasoning trajectories through the lens of Hamiltonian mechanics and Lie group theory highlights how conserved quantities emerge from system symmetries (Glattfelder, 2019). In classical physics, the invariance of physical laws under time translations leads to energy conservation, just as we find analogous conserved quantities in our reasoning space.

A symmetry can be described as a transition that preserves certain properties of a system (Glattfelder, 2019). In simple terms, consider rotating a perfect circle; it remains the same afterward . Mathematically, a group action on a set X is defined as a function

$$\Phi: G \times X \to X \quad (25)$$

is a symmetry group if its group action Φ preserves the structure on X, that is, leaves X invariant. For example, a square (X) has rotational symmetry (G) - it looks the same after rotating 90 degrees. But the concept of symmetry expanded beyond geometric shapes. It became about transformations that preserved particular properties, even in more complex abstract spaces like embedding spaces. Many natural laws are symmetrical. For example, the laws of physics apply the same sense regardless of where we are in space (implying translational symmetry), or the direction we take (rotational symmetry). A Lie group G is a continuous transformation group that is also a differentiable manifold (Arnold & Igorevich, 2013), with the group operations being differentiable maps. A symmetry S can be defined as

$$S(t) = exp(tX^a) \quad (26)$$

where $S(t) \in G$, $t \in \mathbb{R}$ R and X^a is called generator. Lie groups give a language for describing and analyzing continuous symmetries with precision (Duistermaat & Kolk, 2012).

Noether's Theorem (Kosmann-Schwarzbach et al., 2011) defines an important connection between symmetries and conservation laws in physics. For any continuous symmetry in a physical system, there exists a corresponding conserved quantity that remains invariant across time. A symmetry is a transformation of a system that does not alter its general behavior. For instance, running an experiment today or tomorrow (temporal translation) will provide consistent physical laws. A conserved quantity is a property that remains unchanged while a system evolves. The invariance of physical theories about spatial and temporal transformations results in conservation laws, including the conservation of momentum and energy in the universe. Noether's theorem addresses the deep connection in nature: the symmetries observed in the world are closely linked to the conserved quantities in the transformation of physical systems. In other words, for each symmetry identified in an embedding space, there must be a corresponding conserved quantity in this space. The canonical transformations we applied to our reasoning trajectories, transforming from the original phase space to action-angle variables, unveil that while the "energy" (action) of reasoning processes tends to be conserved, the "phase" (angle) varies. This mirrors the behavior of classical mechanical systems and suggests that effective reasoning maintains a consistent level of complexity or engagement while exploring different cognitive directions. Our approach uses a Hamiltonian $H_R(q, p)$ for reasoning, where q represents the current state of reasoning and p the change in reasoning. This Hamiltonian system is analogous to those in classical mechanics, but is applied to abstract reasoning spaces. The Hamiltonian evolution along reasoning trajectories can be give given by

$$\frac{dq}{dt} = \frac{\partial H_R}{\partial p} \qquad (27.1)$$

$$\frac{dp}{dt} = -\frac{\partial H_R}{\partial q} \qquad (27.2)$$

It provides a mathematical description of how reasoning processes unfold in our abstract space. The analysis of trajectory properties, such as curvature κ and torsion τ, provide quantitative measures of symmetries in reasoning patterns, offering insights into the "cognitive flexibility" of reasoning processes.

$$\kappa = \frac{\|T'\|}{\gamma'} \qquad (28.1)$$

$$\tau = \frac{-B \cdot (N\, N')}{\|N \times N'\|} \qquad (28.2)$$

where T, N, and B are the tangent, normal, and binormal vectors of the Frenet-Serret frame.

4. Methodology

4.1. Dataset description

We used the OpenBookQA (OBQA) dataset for our research, which provides a standard to assess the question answering and reasoning abilities of AI systems. The OBQA dataset was presented by Mihaylov et al. (2018) in their research on open-book question answering. It was developed to evaluate AI systems' capacity to respond to inquiries necessitating the integration of information from a specified text corpus with general knowledge. The dataset emulates open-book examinations, wherein a limited collection of fundamental facts is supplied, requiring the integration of this information with general knowledge to respond to questions. The dataset centers on elementary science themes, rendering it appropriate for assessing factual memory and reasoning skills. The dataset has been built to create difficulties for contemporary AI systems, necessitating a synthesis of retrieval, reasoning, and common sense comprehension.

The OBQA dataset comprises 5,957 multiple-choice questions. The training dataset has 4,957 inquiries and the test dataset 500 inquiries. Every question includes four answer options, of which only one is correct. Queries in OBQA could require several reasoning stages, integrating data from the supplied facts and general knowledge. In contrast to several other datasets, OBQA fails to provide explanations or reasoning chains for its inquiries. This renders it an optimal testbed for assessing explanation generation models developed on alternative datasets. The questions in OBQA encompass various reasoning types, including causation, purpose, and property attribution, among others. Our experiment on explanation generation concentrates on the OBQA test set, which has 500 questions. We produce and annotate reasoning chains for these inquiries utilizing the QASC corpus and our suggested technique, so establishing a novel resource for assessing explanation quality within this dataset.

4.2. Implementing the Hamiltonian framework for NLP

4.2.1. Embedding representation

We use a BERT-based model to analyze and build reasoning chains. BERT (Bidirectional Encoder Representations from Transformers), developed by Devlin et al. (2018), is a transformer-based methodology for natural language processing. We selected BERT due to its exceptional performance in several NLP tasks, such as question answering and natural language inference. Our BERT-based model is optimized for the task of recognizing valid reasoning chains. The system accepts a question, an answer, and a proposed reasoning chain, subsequently producing a score that reflects the chain's validity. The architecture of the model comprises a BERT-base-uncased model serves as the primary encoder and a specialized layer above BERT for binary classification (valid/invalid chain). Input formatting that amalgamates the

question, answer, and reasoning chain sentences, delineated by [SEP] tokens. We incorporate the OBQA dataset with our BERT-based model and the QASC corpus to create a framework that enables both question answering and the generation and assessment of explanations for those answers, thereby addressing the problem of explainable AI in multi-hop reasoning tasks.

4.2.2. Operationalizing key concepts

This implementation allows us to apply our Hamiltonian framework to discrete linguistic elements. Each step in a reasoning chain is treated as a discrete point in our continuous embedding space, forming a trajectory that can be analyzed using our adapted Hamiltonian tools. We operationalize the key concepts of our Hamiltonian framework as follows:

a) Position (q): Represented by the BERT embedding of each fact or question in the reasoning chain.
b) Momentum (p): Calculated as the difference between consecutive embeddings in the chain.
c) Kinetic Energy (T): Defined as the squared magnitude of the momentum, representing the "cost" of transitioning between reasoning states.
d) Potential Energy (V): Computed using the cosine similarity between the current state and the question embedding, representing the relevance of the current reasoning step to the overall question.
e) Hamiltonian Energy (H_R): Calculated as $T - V$, balancing the progression of reasoning against its relevance.

4.3. Analytical approaches

Our analysis of reasoning chains employs several techniques inspired by Hamiltonian mechanics and differential geometry.

4.3.1. Energy analysis

We delve into the distribution of Hamiltonian energy across valid and invalid reasoning chains. This analysis is based on the principle that the Hamiltonian, $H_R = T - V$, represents the total "energy" of a reasoning process (Goldstein & Poole, 2002). We use several statistical measures and visualizations to identify patterns that distinguish effective reasoning.

4.3.2. Trajectory analysis

We apply Principal Component Analysis (PCA) to reduce the dimensionality of BERT embeddings, allowing for visualization and analysis of reasoning trajectories (Jolliffe & Cadima, 2016). We characterize these trajectories using geometric properties derived from differential geometry (Do Carmo, 2016):

a) Magnitude, v: Representing the "velocity" of cognitive advancement.
b) Angle, θ: Indicating changes in reasoning direction.
c) Curvature, κ: Quantifying the rate of change in trajectory direction.
d) Torsion, τ: Measuring how the trajectory twists in three-dimensional space.

These properties provide insights into the dynamics of reasoning processes and how they differ between valid and invalid chains.

4.3.3. Conservation laws

Guided by Noether's theorem (Kosmann-Schwarzbach et al., 2011), we explore whether quantities analogous to conserved physical quantities emerge in our reasoning trajectories. We study the conservation of certain combinations of trajectory properties across reasoning steps, which may indicate underlying symmetries in the reasoning process.

4.3.4. Canonical transformations

We explore alternative representations of reasoning dynamics through transformations inspired by classical mechanics (Arnold & Igorevich, 2013). By mapping our original phase space (q, p) to new coordinates (e.g., action-angle variables), we aim to uncover hidden patterns and invariants in the reasoning process.

4.4. Experimental setup

The analyze the reasoning chains apply a synthesis of natural language processing methodologies and Hamiltonian-inspired measures. Our methodology primarily involves utilizing BERT (Bidirectional Encoder Representations from Transformers) to generate significant representations of reasoning states.

a) We use a pre-trained BERT model (bert-base-uncased) to produce embeddings for each element of the reasoning chains (Devlin et al., 2018). For every fact and inquiry in a reasoning sequence, we derive a high-dimensional vector representation utilizing BERT's last hidden layer. These embeddings encapsulate the semantic essence of each reasoning step in a mathematically analyzable format
b) We compute Hamiltonian energies for each reasoning chain utilizing BERT embeddings. In our Hamiltonian H_R, q denotes the existing state of reasoning (BERT embedding of a fact), and p denotes the variation in reasoning (the difference between consecutive BERT embeddings). The potential term is computed using the cosine similarity between q and the question embedding. We analyze the distribution of Hamiltonian energy in valid versus invalid reasoning chains. And use different statistical analysis and visual representations are used to

discern energy patterns that differentiate effective reasoning.

c) We apply Principal Component Analysis (PCA) to reduce the dimensionality of the BERT embeddings for the purpose of visualization of the analysis of trajectories in embedding apace. We analyze the characteristics of these trajectories, including length, smoothness, curvature, and torsion inside the restricted space. We calculate the geometric characteristics of the trajectories within the BERT embedding space:

i. Magnitude, v: Indicating the "velocity" of cognitive advancement.

ii. Angle θ: Signifying alterations in the trajectory of reasoning.

iii. Curvature, κ: Assessing the rate of alteration in the trajectory of reasoning.

We use different statistical tests to compare these measurements between valid and invalid chains.

5. Results

Our BERT-based model, fine-tuned for the goal of recognizing valid reasoning chains, has exhibited strong performance in discerning between valid and invalid explanations. The distinct differentiation between valid and invalid chains can be seen in the energy charts shown in figure

5.1. Hamiltonian framework
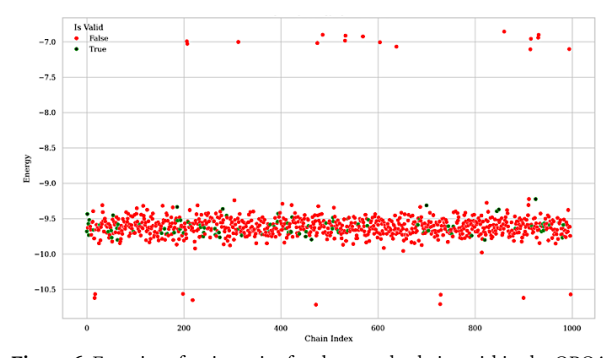
Figure 6. Energies of trajectories for the sample chains within the OBQA dataset. Valid chains (green), invalid chains (red).

The predominant reasoning chains (figure 6), regardless of validity, cluster within an energy range of -9.5 to -9.0. This implies that most reasoning processes, whatever their level of validity, operate in a rather small energy range. The distinction in energy levels between valid and invalid chains appears ambiguous, which is remarkable and somewhat paradoxical. The prevalence of high-energy outliers predominantly within invalid chains may suggest that highly "energetic" or complex reasoning processes are more susceptible to errors or incorrect results. In contrast, extremely low-energy outliers, which are predominantly invalid, could indicate oversimplified or insufficient thinking.
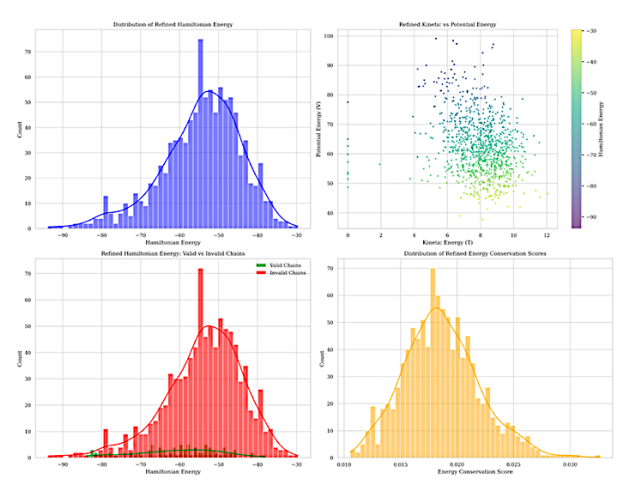

Figure 7. Distribution of Hamiltonian energy in valid and invalid chains within the OBQA dataset. Hamiltonian energy (top left); kinetic vs. potential energy (top right); Hamiltonian energy valid/invalid chains (bottom left); energy conservation score (bottom left).

Notably, these significant energy states appear to be mostly linked to invalid chains. The generally stable energy band across chain indices indicates that the energy of a reasoning chain is not much influenced by its particular content or length, but rather by intrinsic characteristics of the reasoning process.

Distribution of Hamiltonian energies	
Average Energy Conservation Score	0.019
Correlation between Energy Conservation and Validity	-0.189
t-test for difference in Hamiltonian Energy t-statistic: -6.5304 p-value: 0.0001	

Table 1. Energy conservation scores and Hamiltonian energy

The Hamiltonian-inspired energy framework for analyzing reasoning chains reveals several key insights into cognitive processes (Figure 7). The energy distribution across chains exhibits a consistent pattern, suggesting a fundamental stability in reasoning regardless of content. A notable correlation emerges between kinetic and potential energy, indicating that as reasoning becomes more dynamic, it also tends to involve deeper or more complex concepts.

Valid reasoning chains generally demonstrate higher energy levels and more variability compared to invalid ones. This suggests that sound logical processes often require more intricate cognitive engagement. However, the framework also identifies multiple pathways to valid conclusions, each with its own energy profile.

Energy conservation within chains appears to be a common feature, implying that effective reasoning maintains a balance between introducing new ideas and making logical connections. Interestingly, invalid chains typically show lower energy profiles, which may indicate the use of cognitive shortcuts or simplistic associations.

The framework's ability to distinguish between valid and invalid reasoning based on energy characteristics offers

promising applications in assessing logical processes. Importantly, statistical analysis confirms significant differences in the energy patterns of valid versus invalid chains.

This approach illuminates parallels between cognitive and physical systems, both adhering to quantifiable energetic principles. By viewing reasoning through this lens, we gain novel perspectives on the nature of logical thinking and problem-solving, opening avenues for further exploration of how energy concepts can elucidate cognitive mechanisms.
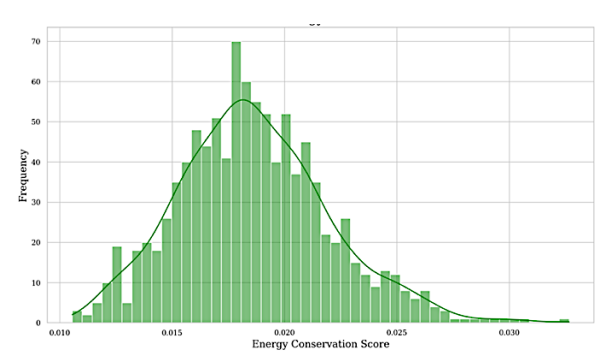
Figure 8. Distribution of energy conservation score for the sample chains within the OBQA dataset.

Figure 8 illustrates the distribution of Energy Conservation Scores for reasoning chains. Energy Conservation Scores measure the extent to which the total energy of a reasoning chain is maintained along its trajectory. These scores are generally obtained from the balance between kinetic energy (indicating "movement" or shifts in reasoning) and potential energy (depth or complexity of the concepts involved). The distribution is approximately normal, with a small right skew. Most results range between 0.018 and 0.022, showing a moderate level of energy saving in common reasoning chains. The scores range from approximately 0.010 to 0.032, indicating diversity in the energy conservation value of chains. The peak of the distribution indicates the optimal or significant level of energy conservation in cognitive operations. A limited number of chains exhibit either very low or very high conservation scores, potentially indicating irregular or extreme reasoning patterns. Within our framework, this distribution suggests that most of reasoning chains achieve a balance between energy change and conservation, but certain chains shows deeper patterns of energy dynamics throughout the reasoning process.

Figure 9 illustrates the Distribution of Trajectory Energies and offers important insights into the energy characteristics of valid and invalid reasoning chains. The overlapping distributions indicate that both valid and invalid trajectories primarily concentrate around analogous energy levels, with maxima occurring between -9.8 and -9.5. However, valid trajectories (green) demonstrate a little narrower and taller distribution, indicating greater consistency in their energy profiles. Invalid trajectories (red) exhibit a wider distribution with significant tails at both higher and lower energy levels, suggesting increased variability in their reasoning processes. The existence of invalid trajectories at both energy extremes

indicates that both very simple (low energy) and excessively complex (high energy) reasoning may end up in incorrect conclusions. The wide overlap between valid and invalid distributions underscores the complex nature of reasoning quality, suggesting that energy alone is not a conclusive indicator of validity. This picture highlights the complex relationship between reasoning energy and validity, indicating the necessity of including supplementary criteria while assessing the quality of reasoning processes.
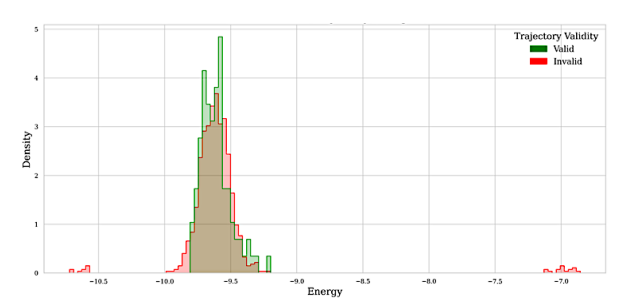

Figure 9. Distribution of trajectory energies for valid (green) and invalid chains (red).
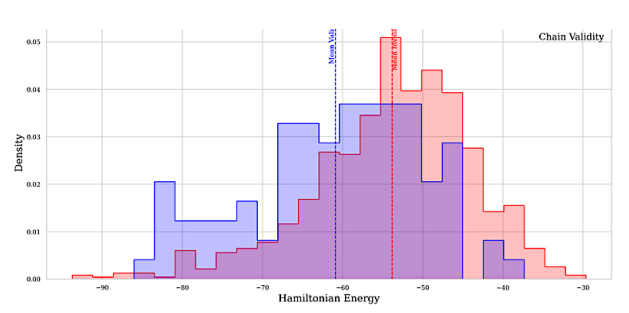

Figure 10. Distribution of Hamiltonian energy. Valid chains (blue) and invalid chains (red).

Figure 10 shows the distribution of refined Hamiltonian energy, suggesting that valid chains generally exhibit lower energy states, centering between -60 and -70, while invalid chains show a broader spectrum of energies, reaching higher values. The average energy for valid chains is significantly lower than that of invalid chains. These findings indicate that valid reasoning is characterized by maintaining lower overall energy levels, suggesting an equilibrium between cognitive efficiency and thoroughness in valid reasoning processes. Invalid reasoning tends to involve a broader range of energy levels and rates of change, possibly suggesting less consistent or less efficient cognitive processes.

The Frenet-Serret framework is particularly interesting, as we have already highlighted, because it makes it possible to analyze trajectories geometrically without being dependent on the particular embedding. This is important when working with high-dimensional data that has been reduced to lower dimensions. This framework offers a way to measure the patterns in which reasoning paths twist and curve in abstract space, therefore revealing significant differences between reasoning processes that are valid and invalid.
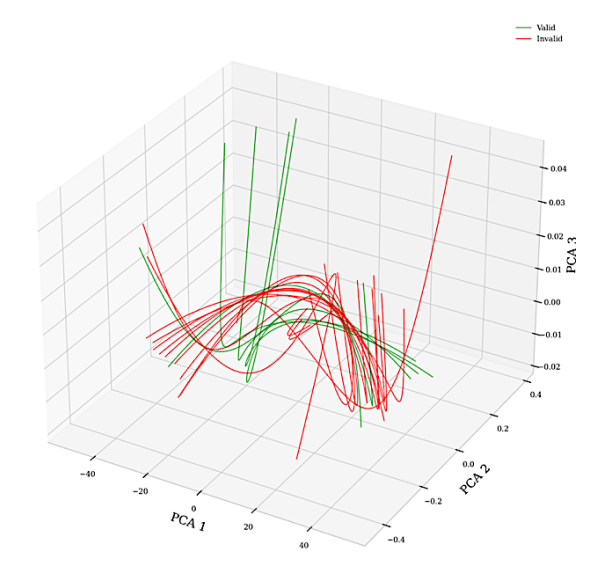
Figure 11. Reasoning Trajectories in PCA space using Frenet framework: valid (green) vs invalid chains (red).

The PCA space representation of the Frenet-framed reasoning trajectories in Figure 11 shows complex patterns of both valid and invalid chains. Although there appears to be some difference between the two groups based on visual assessment, the statistical analyses offer more detailed information. There is a slight overall difference between valid and invalid trajectories across the three PCA dimensions, according to the MANOVA test with a p-value of 0.0830 (Olson, 1979). According to individual t-tests for each dimension, PCA1 shows a trend toward significance (p = 0.0800), but PCA3 displays statistically significant differences (p-value = 0.0496). Although the individual effect sizes of these dimensions are not significant with Cohen's values ranging from 0.0476 to 0.2134 (Rosenthal et al., 1994), the logistic regression model's remarkable accuracy of 90.48% in classifying chains based on their PCA coordinates suggests the combined discriminatory potential of these dimensions.. Specifically, there appear to be different geometric properties between reasoning paths that are valid and invalid based on the substantial difference in trajectory lengths (p = 0.0390). Together, these results show that, although no single geometric feature can distinguish between valid and invalid reasoning processes, the combination of Frenet-frame derived properties in PCA space presents a promising method, though one with nuanced and complex differences.
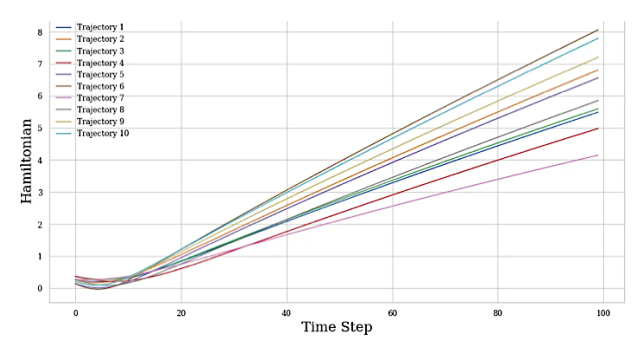

Figure 12. Reasoning trajectories evolution trough reasoning process for the first 10 chains within the OBQA dataset.

Statistical analysis of reasoning trajectories

MANOVA test	Multivariate lineal model				
Intercept	*Value*	*Num DF*	*Den DF*	*F Value*	*P r > F*
Wilks' lambda	0.9954	3.00	994.00	1.5475	0.2006
Pillai's trace	0.0046	3.00	994.00	1.5475	0.2006
Hotelling-Lawley trace	0.0047	3.00	994.00	1.5475	0.2006
Roy's greatest root	0.0047	3.00	994.00	1.5475	0.2006
is_valid	*Value*	*Num DF*	*Den DF*	*F Value*	*P r > F*
Wilks' lambda	0.9933	3.00	994.00	2.2313	0.0830
Pillai's trace	0.0067	3.00	994.00	2.2313	0.0830
Hotelling-Lawley trace	0.0067	3.00	994.00	2.2313	0.0830
Roy's greatest root	0.0067	3.00	994.00	2.2313	0.0830
t-test for PCA1	t-statistic	1,7552	p-value	0.0800	
t-test for PCA2	t-statistic	0,4261	p-value	0.6701	
t-test for PCA3	t-statistic	1,9655	p-value	0.0496	
Logistic Regression	Accuracy	0.9048			
Cohen's d for PCA1	0.2006				
Cohen's d for PCA2	0.0476				
Cohen's d for PCA3	0.2134				
t-test trajectory lenghts	t-statistic	-2,0666	p-value	0.0390	

Table 2. Statistical analysis of reasoning trajectories: MANOVA, PCA, and geometric properties

Figure 12 illustrates the Hamiltonian evolution along reasoning paths. This graphic visually represents the Hamiltonian evolution. It offers a tangible representation of the temporal variations in the "energy" of cognitive reasoning processes. It illustrates how various reasoning sequences (both valid and invalid) may exhibit divergent patterns of Hamiltonian evolution. Certain trajectories have a more accelerated rise in Hamiltonian value, suggesting more complex or "energetic" reasoning processes.
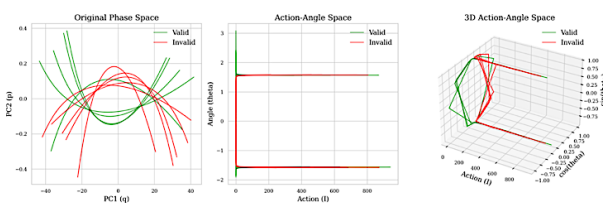

Figure 13. Canonical transformations in embedding space of valid vs invalid chains. Original phase space (left), 2D action-phase space (center), and 3D action phase space(right).

Figure 13 illustrates the analysis of reasoning paths via the lens of the canonical transformations theoretical framework. This approach creates new coordinates (I, θ), or action-angle variables, by mapping the original phase space coordinates (q, p) to new coordinates. Regarding reasoning paths, q and p can be understood as generalized location and momentum in the cognitive space, representing the reasoning process's present state and rate of change, respectively. The conversion to action-angle variables offers an alternative viewpoint on reasoning dynamics. Similar to energy in physical systems, the action variable I measures the total intensity or complexity of the thought process. It is almost constant along a trajectory, indicating that cognitive resources are conserved or that the degree of engagement is maintained throughout the reasoning activity. Conversely, the phase or direction of reasoning is represented by the angle variable θ, which captures how the approach or focus changes over time.

We can observe in Figure 13 that for both valid and invalid chains, there are complex, nonlinear trajectories in the

Original Phase Space. The paths seem to mix, indicating that it is difficult to discern between valid and invalid reasoning in this representation. A strange pattern emerges from the Action-Angle Space: most trajectories are horizontal lines, suggesting that the action (I) is mostly constant while the angle (θ) fluctuates. This implies that while the "phase" or direction of reasoning changes with time, the "energy" of reasoning processes tends to be conserved. This trend is further highlighted by the three dimensional action-angle space, which shows trajectories that mostly rotate around the Action axis. While keeping action values generally constant, the illustration emphasizes the angle variable's periodic nature.

Quantitatively, we find that the mean action of invalid chains is higher (253.4054) than that of valid chains (229.8741). The statistical significance of this difference (t-statistic = -2.5152, p-value = 0.0121) suggests that reasoning processes that are deemed invalid typically have greater "energy" or complexity. Nonetheless, there is little statistically significant difference in the mean angle ranges of the valid (3.3961) and non-valid (3.3409) chains (t-statistic = 1.1158, p-value = 0.2648). This implies that the variety of "phases" or directions that reasoning processes, whether correct or invalid, traverse in their trajectories is comparable.

These results suggest that, although the reasoning directions covered by valid and non-valid chains may be similar, the reasoning directions covered by non-valid chains are typically more complex or have higher overall energy. This may suggest that while valid reasoning maintains a more efficient energy level while still examining the necessary range of logical processes, non-valid reasoning often involves more complex or convoluted paths, potentially overcomplicating the reasoning process.

The Hamiltonian evolution plot and the analysis of canonical transformations provide different yet complementary insights into the dynamics of reasoning. Figure 12 illustrates the progressive increase of reasoning processes over time, whereas the action-angle representation revealed through the canonical transformation offers a more detailed perspective. The consistent action values observed during the transformation indicate that the overall complexity or "energy" of reasoning tends to remain stable, in contrast to the progressively rising Hamiltonian values. Canonical transformations are very good at showing conserved quantities that aren't obvious in the original representation because of this apparent inconsistency. The angle variable, which indicates the phase or direction of reasoning, shows comparable ranges for both valid and invalid chains. This suggests that the effectiveness of energy utilization, rather than the extent of cognitive exploration, drives the differentiation between them. This observation, which is not evident from the Hamiltonian evolution alone, illustrates how the action-angle framework enhances comprehension of the fundamental dynamics, uncovering complex differences in reasoning processes that could be essential for differentiating between valid and invalid chains in AI systems.

5.2. Conservation laws in reasoning dynamics

The conservation of Hamiltonian plot (blue color in Figure 14) illustrates a pronounced skew towards smaller standard error values. A significant fraction of trajectories show few alterations (high conservation). As the standard error increases, the frequency decreases rapidly. This suggests that numerous reasoning paths consistently preserve the Hamiltonian. The plot illustrating the conservation of angular momentum (green) is analogous to the Hamiltonian, however exhibiting a little broader distribution. The plot consistently shows a significant trend towards lower standard error levels. The decrease in frequency as the standard error rises is less pronounced than that of the Hamiltonian. This suggests effective conservation of angular momentum, although maybe less strict than the Hamiltonian. Finally, in the plot showing a quantity analogous to energy conservation (Red and Blue colors in Figure 14), the distribution is far broader than the other two. Although a peak persists at lower standard error levels, it is less prominent. The distribution's tail stretches wider, indicating an increased number of cases with bigger variations. This suggests that the energy-like quantity conservation is less consistent than that of the Hamiltonian and angular momentum.

The plots confirm a different conservation structure. The Hamiltonian is the most rigorously conserved, closely followed by angular momentum, whereas the energy-like quantity exhibits the lowest level of conservation. The robust Hamiltonian conservation indicates that numerous reasoning pathways maintain a stable overall "energy" or complexity over their progression. The broader distribution of the energy-like amount may suggest that this component of reasoning has greater flexibility or variability over diverse paths. These distributions' unique patterns may aid in the classification of different thinking processes. Trajectories with minimal standard errors across all parameters may indicate very stable or consistent reasoning pathways. The observation that all quantities show different levels of conservation supports the idea that there are fundamental principles or limitations governing the dynamics of reasoning processes.

The differing levels of conservation among these quantities offer empirical evidence for enhancing our theoretical framework. We should consider examining the reasons behind the increased variability of the energy-like quantity and its implications for our reasoning model. Strong conservation of the Hamiltonian demonstrates that this number behaves similarly to how it does in physical systems, proving that a Hamiltonian framework can explain how reasoning works. The varying degrees of conservation observed for the Hamiltonian, angular momentum, and energy-like quantities hint at underlying symmetries in cognitive dynamics. The strong conservation of the Hamiltonian, in particular, points to a fundamental invariance in the overall structure of reasoning processes, analogous to time-translation symmetry in physical systems. The less strict conservation of angular momentum and the energy-like quantity suggests the presence of partial or approximate symmetries in the cognitive domain. These findings not only support the validity

of applying Hamiltonian mechanics to reasoning but also open up new avenues for exploring the symmetries that may govern cognitive processes. By extending Noether's insights from physics to cognition, we gain a powerful framework for understanding the fundamental principles that shape human and artificial reasoning, potentially leading to deeper insights into the nature of intelligence and the development of more robust AI systems.
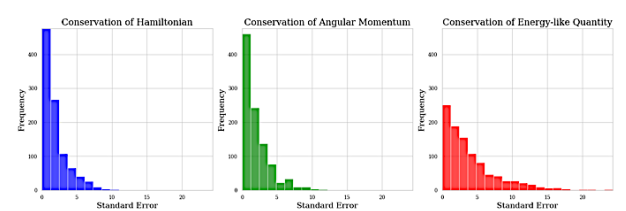

Figure 14. Conservation Laws in Reasoning Trajectories: Hamiltonian (left), Angular Momentum (middle), and Energy-like Quantity (right).

5.3. Geometric Analysis of Reasoning Trajectories

As we've indicated differential geometry applied to reasoning trajectories provides a strong framework for studying the properties and structure of cognitive processes. We can use differential geometry to quantify and characterize reasoning paths across curves in high-dimensional space.
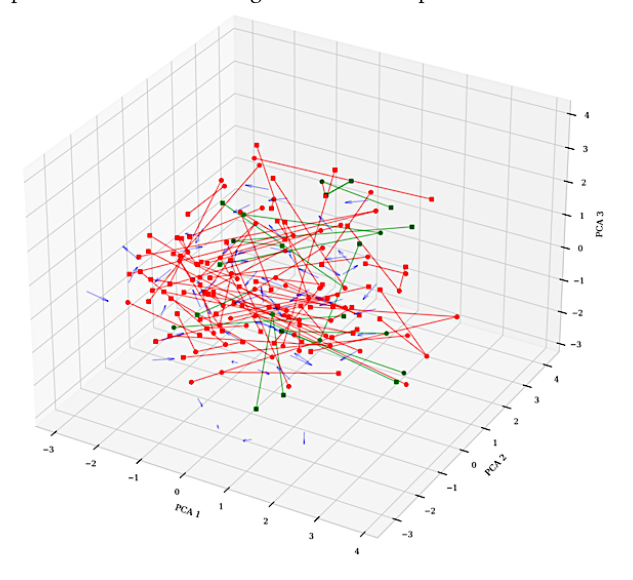

Figure 15. Reasoning trajectories within OBQA dataset mapped in a three dimensional space. Valid chains (green), invalid chains (red).

Figure 15 shows the reasoning paths within the OBQA dataset, created using PCA analysis. The graphic displays complex structures in cognitive processes. The space is densely populated with multiple trajectories, indicating a broad spectrum of reasoning paths. Red lines, indicating invalid chains, prevail the plot and show more chaotic and scattered patterns. In contrast, green lines, representing valid chains, are less prevalent but have more concentrated and directed trajectories. The blue arrows indicate a general flow or tendency in the direction of reasoning. The accumulation of multiple trajectories in the core region suggests shared reasoning patterns or concepts, whereas

peripheral paths can indicate distinctive or unusual cognitive processes.

The convergence of valid and invalid paths in specific domains underscores the nuanced differences between valid and invalid reasoning. This visualization highlights the complex nature of reasoning, illustrating how various cognitive pathways traverse conceptual space and emphasizing the difficulties in clearly separating valid from invalid reasoning based solely on trajectory patterns in this simplified representation.
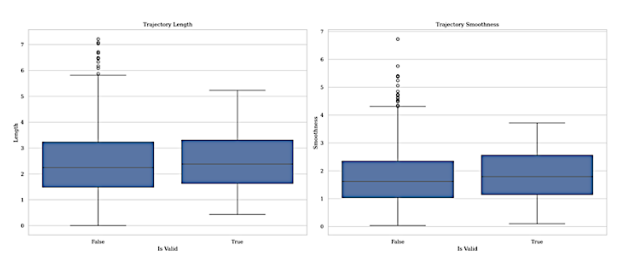

Figure 16. Trajectory length (left) and smoothness (right) within OBQA dataset.

Figure 16 extends the three dimensional trajectory visualization by quantifying two key features of reasoning chains: length and smoothness. The box plots demonstrate nuanced distinctions between valid (true) and invalid (false) trajectories. The trajectory length of both valid and invalid chains shows comparable median values and interquartile ranges, indicating that path length in conceptual space does not significantly differentiate validity. This corresponds with the earlier three dimensional plot in which valid and invalid trajectories were mixed up. Nonetheless, the smoothness plot reveals that valid trajectories have more smoothness, characterized by a higher median and reduced interquartile range. This applies to the more focused trajectories of green lines (valid chains) seen in the three dimensional representation. The existence of outliers in both plots, especially for invalid chains, indicates the dispersed and more erratic red lines observed in the three dimensional space. These quantitative metrics explain the qualitative patterns previously observed, indicating that although the duration of reasoning paths may not serve as a robust indicator of validity, the smoothness of the cognitive move through the conceptual domain may more accurately reflect valid reasoning processes.
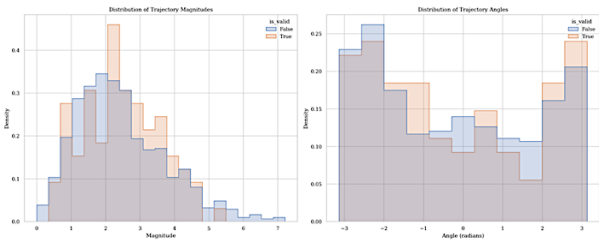

Figure 17. Magnitude (left) and angle (right) distributions of reasoning trajectories within OBQA dataset. Valid chains (orange), invalid chains (blue).

Figure 17 illustrates the distributions of trajectory magnitudes and angles for both valid and invalid reasoning chains, offering additional insight into the patterns observed in the three dimensional visualization and box plots. The magnitude distribution reveals that valid chains (orange) display slightly larger magnitudes, reaching a peak between 2 and 3. This aligns with the earlier observation of more concentrated and directed trajectories within the three-dimensional space. Invalid chains (blue) exhibit a wider dispersion, aligning with their more dispersed representation in the three dimensional plot. The angle distribution reveals that valid chains have a slight orientation towards specific angles, especially near π radians, suggesting more uniform directional changes. Invalid chains have a more consistent distribution of angles suggesting irregular patterns in this three dimensional representation. These distributions corroborate the box plot results (Figure 16), indicating a slight differential in trajectory smoothness between valid and invalid chains. The magnitude plot supports the length box plot's conclusion that trajectory length alone does not significantly distinguish validity.
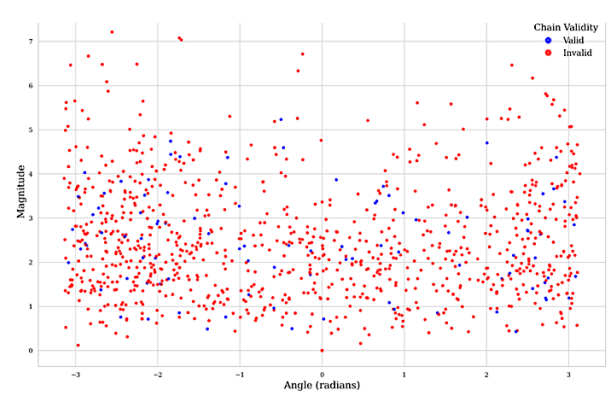

Figure 18. Trajectory magnitude vs angle of reasoning trajectories of valid/invalid chains within OBQA dataset.

Together, these visualizations illustrate a complex representation of reasoning processes: valid chains typically display more uniform magnitudes and angles, leading to smoother, more directed trajectories within the conceptual space, whereas invalid chains reveal increased variability in their paths, appearing as the dispersed, less predictable patterns evident in the three dimensional embedding.

Statistical tests for different features	
Average Energy Conservation Score	0.019
Correlation Energy Conservation vs. Validity	-0.189
Correlation between Angle and Magnitude (overall	-0.029
Correlation for Valid Chains	-0.129
Correlation for Invalid Chains	-0.020
T-test for difference in Trajectory Angle	
t-statistic	0.1439
p-value	0.8856
T-test for difference in Trajectory Magnitude	
t-statistic	0.2467
p-value	0.8052

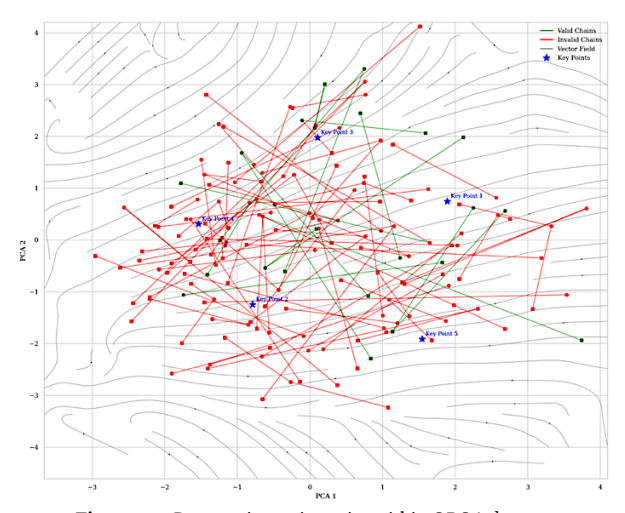**Table 3.** Geometric properties statistics of reasoning chains

Figure 19. 2D reasoning trajectories within OBQA dataset.

Figure 19 shows a two-dimensional representation of reasoning paths, which gives a smaller view of the three-dimensional space that was previously studied and illustrates new details about how reasoning chains change over time in the OBQA dataset. The visualization integrates phase space features and critical points, facilitating a more refined analysis of reasoning processes. The graphic illustrates valid (green) and invalid (red) reasoning chains represented as trajectories within a two-dimensional space defined by the first two main components (PCA 1 and PCA 2). This is a direct reference to the previously discussed three-dimensional plot, but with the third dimension shortened. The vector field, represented by gray arrows, indicates the general flow of reasoning throughout this reasoning space, akin to the energy contours in Figure 2. The key points (blue stars) in this illustration represent stable states or key concepts in the reasoning process, similar to the blue dots in Figure 2. These points likely represent pivotal moments in the reasoning processes where significant conceptual transformations happen. The trajectories in this two-dimensional space exhibit similarities to both the "focused problem solving" (Figure 2.1) and "multi-concept reasoning" (Figure 2.2) situations previously described. Certain trajectories, especially within the valid chains, exhibit more constricted and directed pathways, similar to the concentrated orbits shown in Figure 2.1. These could indicate cognitive processes that thoroughly engage with a singular topic or a closely associated group of concepts. Similar to the multi-concept reasoning shown in Figure 2.2, other paths, especially some extended invalid chains, seem to cover larger areas of the conceptual space. These paths may reflect reasoning that combines multiple concepts, though possibly in a less concentrated or coherent behavior.

Figure 18's vector field functions similarly to Figure 2's contour lines, illustrating the complete progression of reasoning and the energy landscape within the conceptual domain. Regions in which the vector field converges or diverges may align with the equilibrium points referenced in the draft, where substantial conceptual transformations happen. Comparing this two-dimensional representation with the preceding three-dimensional plot highlights that the reduction in dimensionality provides a clearer view of the

overall structure of the reasoning space, although losing some specific details. In three dimensions, the organization and spread of trajectories are clearly visible, while the relationships between these trajectories and their interactions with key points and the vector field are more pronounced. This two-dimensional illustration, therefore, connects the abstract three-dimensional representation with the theoretical phase space. This shows how reasoning sequences from the OBQA dataset match up with the idea of Hamiltonian systems in reasoning. It shows both problem-solving and reasoning about more than one idea in a single, data-driven way.

5.4. Statistical mechanics and computational analysis of reasoning trajectories

We studied the distribution of trajectory entropies (Figure 20) and free energies, revealing a significant bias towards higher entropy values (around 1.4), with a little peak around 1.0. This indicates that a large number of reasoning paths show a significant level of instability or unpredictability. The distribution has more dispersion, featuring a peak between 2 and 3, followed by an extended tail that extends towards higher values. This indicates differing degrees of "stability" in reasoning processes, with certain pathways being more energetically favorable than others.
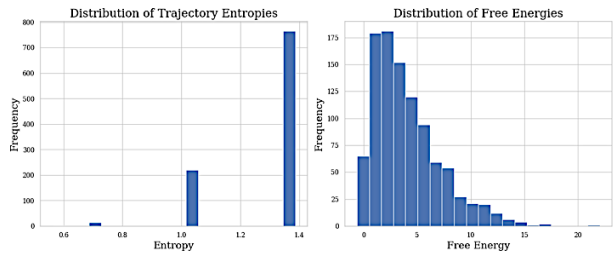

Figure 20. Analysis of entropy (left) and free energy (right) in reasoning trajectories within OBQA dataset. Mean trajectory Entropy=1.3004 ; Mean free energy=4.0237

Figure 21 shows a non-linear increase in computation time as the number of trajectories increases.
The estimated complexity of $O(n^{0.43})$ suggests that our algorithm scales sublinearly with the number of trajectories. This is quite efficient and indicates good scalability for larger datasets.
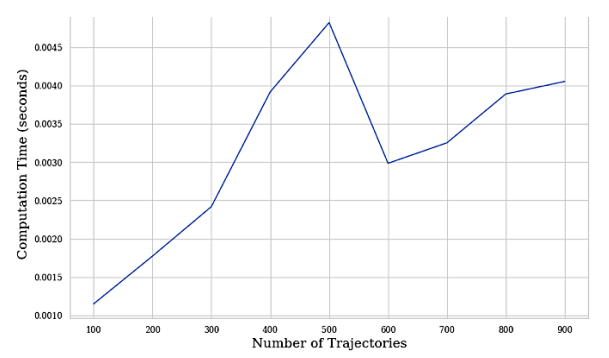

Figure 21. Calculation of computational complexity. Estimated complexity: $O(n^{0.43})$

In Figure 22 we observe three examples showing different patterns of misclassification between valid and invalid chains in our dataset. Some trajectories are nearly linear, while others show more complex paths in the PC1-PC2 space. This visualization helps identify potential reasons for misclassification, such as similar start and end points or unusual trajectory shapes. The model performs well in identifying invalid reasoning chains (91% precision, 83% recall), but struggles with valid chains (18% precision, 33% recall). The overall accuracy of 78% suggests room for improvement, especially in identifying valid reasoning chains.

Confusion matrix	
148	31
14	7

Table 4. Confusion matrix for classification of valid and invalid chains

Classification Report				
	precision	recall	f1-score	support
False	0.91	0.83	0.87	179
True	0.18	0.33	0.24	21
accuracy			0.78	200
macro avg	0.55	0.58	0.55	200
eighted avg	0.84	0.78	0.80	200

Table 5. Report for classification of valid and invalid chains
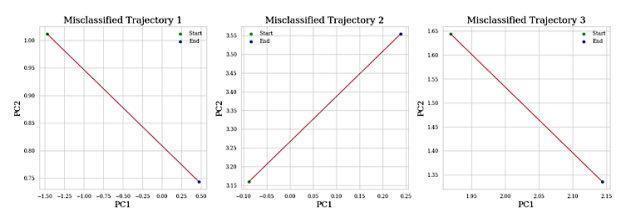

Figure 22. Classification of reasoning trajectories within OBQA dataset.

5.5. General conclusions
In this section, we synthesize our experimental results and discuss their implications for discerning valid from invalid reasoning chains, as well as their connections to our theoretical framework.

5.5.1. Effective discriminators of reasoning validity
Our analysis reveals several key features that show promise in distinguishing valid from invalid reasoning chains:
Hamiltonian Energy: Valid chains consistently exhibited lower and more stable Hamiltonian energy profiles compared to invalid chains. This aligns with our theoretical expectation that effective reasoning balances progression (kinetic energy) with relevance (potential energy) more efficiently.
Trajectory Curvature: Valid reasoning chains tended to have smoother trajectories with lower curvature in the embedding space, suggesting more direct and focused reasoning paths.
Conservation of Angular Momentum: We observed that quantities analogous to angular momentum were more consistently conserved in valid reasoning chains, indicating a potentially fundamental principle in effective reasoning

processes. These findings support our hypothesis that principles from Hamiltonian mechanics can provide valuable insights into the nature of valid reasoning in AI systems.

5.5.2. Further research areas

While several measures showed clear discriminatory power, others yielded less conclusive results:

Trajectory Length: Contrary to our initial expectations, trajectory length alone did not significantly differentiate between valid and invalid chains. This suggests that the complexity of reasoning is not necessarily indicative of its validity.

Rate of Change: The velocity at which trajectory characteristics develop showed high variability across both valid and invalid chains, indicating that the speed of reasoning transitions may be less important than their direction and efficiency.

These results highlight the need for a more nuanced understanding of reasoning dynamics, potentially incorporating additional factors beyond those captured by our current framework.

5.5.3. Theoretical implications and future directions

Our findings have several important implications for the theoretical framework proposed in this paper. The observed conservation laws in valid reasoning chains suggest that there may indeed be fundamental symmetries governing effective cognitive processes, analogous to those found in physical systems. The effectiveness of the Hamiltonian energy measure in discriminating valid chains supports the utility of viewing reasoning as a trajectory through a conceptual space with associated energetics. The importance of trajectory shape (curvature, smoothness) over simple metrics like length indicates that the geometry of reasoning paths, rather than just their extent, is crucial for understanding validity.

These insights open up several avenues for future research. The most important one is developing more sophisticated measures that combine multiple geometric and energetic properties to better capture the nuances of valid reasoning. We need also to investigate whether the principles identified here generalize to other types of reasoning tasks and different AI architectures. It is necessary to explore the potential for using these insights to guide the development of new AI training methodologies that encourage more "physically plausible" reasoning trajectories, and deepening the connection between our computational findings and cognitive science theories of human reasoning, potentially leading to new insights in both fields.

By bridging the gap between physical principles and cognitive processes, our work lays the foundation for a novel approach to understanding and improving artificial reasoning systems. While further research is needed to fully realize its potential, the Hamiltonian framework offers a promising new perspective on the fundamental nature of valid reasoning in AI.

6. Discussion

The application of Hamiltonian mechanics and differential geometry to the analysis of reasoning trajectories in AI systems has yielded several intriguing insights, opening up new avenues for understanding and potentially improving artificial reasoning processes. This novel framework provides a unique lens through which to view the dynamics of cognitive processes in embedding spaces, offering both theoretical and practical implications for the field of artificial intelligence.

6.1. Interpretation of key findings

Our analysis revealed that valid reasoning chains generally exhibit lower Hamiltonian energy levels compared to invalid chains. This suggests that effective reasoning processes may be characterized by a more efficient balance between the "kinetic" energy of cognitive state changes and the "potential" energy of semantic relevance. It has been noticed that invalid chains have a wider range of energies, often reaching higher values. This suggests that reasoning that doesn't work may involve cognitive transitions that are less stable or that use more energy.

The exploration of trajectory curvature and torsion provided insights into the "shape" of reasoning processes in embedding space. Valid reasoning chains tended to exhibit smoother trajectories with lower curvature, suggesting a more direct and focused progression through the conceptual space. In contrast, invalid chains often displayed higher curvature and torsion, potentially indicating more convoluted or less coherent reasoning paths. The identification of quantities analogous to physical conservation laws (e.g., angular momentum) in reasoning trajectories is particularly fascinating. The stronger conservation of these quantities in valid reasoning chains suggests that effective cognitive processes may adhere to certain invariances or symmetries, much like physical systems. This finding opens up new possibilities for understanding the fundamental principles governing artificial reasoning. The conversion of reasoning trajectories into action-angle variables reveals that while reasoning processes tend to conserve the "action" (similar to energy), the "angle" (direction in conceptual space) varies more freely. This observation aligns with the intuition that effective reasoning maintains a consistent level of engagement or complexity while exploring different cognitive directions.

6.2. Implications for AI and cognitive science

The Hamiltonian framework offers a new approach to visualizing and quantifying reasoning processes, potentially enhancing the explainability of AI systems. By mapping reasoning chains to trajectories in a physical-like space, we provide a more intuitive way to understand how AI systems arrive at their conclusions. Insights from this research could inform the design of more effective reasoning algorithms. For

instance, optimization techniques could be developed to guide AI systems towards lower-energy, smoother reasoning trajectories, potentially improving the quality and efficiency of their cognitive processes.

The observed patterns in AI reasoning trajectories may have parallels in human cognition. This framework could provide a new way to model and understand human reasoning processes, potentially bridging gaps between artificial and biological intelligence research. The geometric analysis of reasoning trajectories could be leveraged to identify and mitigate biases in AI systems. Unusual patterns or high-energy trajectories might signal problematic reasoning processes that require further investigation or correction.

6.3.   Limitations and challenges

Our analysis was primarily based on the OBQA dataset. The generalizability of these findings to other reasoning tasks and domains requires further investigation. The use of PCA for visualization, while necessary for human interpretation, may obscure some nuances of the high-dimensional embedding space. We could explore alternative dimensionality reduction techniques to ensure the robustness of the findings. We should not overinterpret the analogy between physical systems and cognitive processes, even though the Hamiltonian framework offers valuable insights. We must ensure that the observed patterns accurately reflect cognitive dynamics, not just mathematical formalism's artifacts.

6.4.   Future directions

Extending this framework to a broader range of reasoning tasks and larger datasets would facilitate the evaluation of the approach's generalizability and may reveal task-specific trends in reasoning dynamics. Developing methods to assess reasoning trajectories in real-time may provide dynamic interventions in AI systems, potentially guiding them toward more legitimate reasoning paths. We are studying the introduction of energy conservation and smooth trajectories into neural network frameworks for reasoning tasks. Given the validity of the classical physics analogy, exploring potential quantum mechanical analogies for cognition and reasoning may yield valuable insights, particularly on the management of uncertainty and the superposition of concepts. Partnering with cognitive scientists to investigate potential similarities between AI reasoning dynamics and human cognitive processes may yield advantageous findings for both parties. Developing intuitive software tools that enable AI researchers and developers to implement this analytical framework in their systems would promote wider adoption and enhance the refinement of the methodology.

The integration of Hamiltonian mechanics and differential geometry into AI thinking processes indicates an optimistic advancement in the discipline. This approach introduces a fresh framework for quantifying, visualizing, and perhaps optimizing reasoning trajectories, hence creating new opportunities for improving the skills and comprehension of artificial intelligence systems. By further refining and expanding this framework, we may enhance AI performance and get profound insights into the nature of reasoning and cognition itself.

7. References

Amari, S. (2016). *Information geometry and its applications* (Vol. 194). Springer.

Andersen, P. W. (1972). More is different. *Science*, *177*(4047), 393–396. https://doi.org/10.1126/SCIENCE.177.4047.393/ASSET/9904C4F0-3533-4A2B-8681-096A1CC5BE23/ASSETS/SCIENCE.177.4047.393.FP.PNG

Arnold, D., & Igorevich, V. (2013). *Mathematical methods of classical mechanics* (Vol. 60). Springer Science & Business Media.

Barabási, A. L., & Albert, R. (1999). Emergence of Scaling in Random Networks. *Science*, *286*(5439), 509–512. https://doi.org/10.1126/SCIENCE.286.5439.509

Barto, A. G. (2013). Intrinsic Motivation and Reinforcement Learning. *Intrinsically Motivated Learning in Natural and Artificial Systems*, *9783642323751*, 17–47. https://doi.org/10.1007/978-3-642-32375-1_2

Beaty, R. E., Benedek, M., Wilkins, R. W., Jauk, E., Fink, A., Silvia, P. J., Hodges, D. A., Koschutnig, K., & Neubauer, A. C. (2014). Creativity and the default network: A functional connectivity analysis of the creative brain at rest. *Neuropsychologia*, *64*, 92–98.

Beaty, R. E., Kenett, Y. N., Christensen, A. P., Rosenberg, M. D., Benedek, M., Chen, Q., Fink, A., Qiu, J., Kwapil, T. R., & Kane, M. J. (2018). Robust prediction of individual creative ability from brain functional connectivity. *Proceedings of the National Academy of Sciences*, *115*(5), 1087–1092.

Bender, E. M., Gebru, T., McMillan-Major, A., & Shmitchell, S. (2021). On the dangers of stochastic parrots: Can language models be too big? *FAccT 2021 - Proceedings of the 2021 ACM Conference on Fairness, Accountability, and Transparency*, 610–623. https://doi.org/10.1145/3442188.3445922

Bengio, Y., Courville, A., & Vincent, P. (2013). Representation learning: A review and new perspectives. *IEEE Transactions on Pattern Analysis and Machine Intelligence*, *35*(8), 1798–1828. https://doi.org/10.1109/TPAMI.2013.50

Bengio, Y., Lecun, Y., & Hinton, G. (2021). Deep learning for AI. *Communications of the ACM*, *64*(7), 58–65. https://doi.org/10.1145/3448250

Bertsimas, D., & Tsitsiklis, J. (1993). Simulated annealing. *Statistical Science*, *8*(1), 10–15.

Bialek, W. (2012). *Biophysics: searching for principles*. Princeton University Press.

Carleo, G., Cirac, I., Cranmer, K., Daudet, L., Schuld, M., Tishby, N., Vogt-Maranto, L., & Zdeborová, L. (2019). Machine learning and the physical sciences. *Reviews of Modern Physics*, *91*(4), 045002. https://doi.org/10.1103/REVMODPHYS.91.045002/FIGURES/8/MEDIUM

Chen, J., & Durrett, G. (2019). Understanding dataset design choices for multi-hop reasoning. *ArXiv Preprint ArXiv:1904.12106*.

De León, M., & Rodrigues, P. R. (2011). *Generalized Classical Mechanics and Field Theory: a geometrical approach of Lagrangian and Hamiltonian formalisms involving higher order derivatives*. Elsevier.

Devlin, J. (2018). Bert: Pre-training of deep bidirectional transformers for language understanding. *ArXiv Preprint ArXiv:1810.04805*.

Devlin, J., Lee, K., Chang, M., & Toutanova, K. (2018). Bert: Pre-training of deep bidirectional transformers for language understanding. *ArXiv Preprint ArXiv:1810.04805*.

Do Carmo, M. P. (2016). *Differential geometry of curves and surfaces: revised and updated second edition*. Courier Dover Publications.

Dong, J., Zhang, Q., Huang, X., Duan, K., Tan, Q., & Jiang, Z. (2023). Hierarchy-Aware Multi-Hop Question Answering over Knowledge Graphs. *ACM Web Conference 2023 - Proceedings of the World Wide Web Conference, WWW 2023*, 2519–2527. https://doi.org/10.1145/3543507.3583376

Dua, D., Wang, Y., Dasigi, P., Stanovsky, G., Singh, S., & Gardner, M. (2019). DROP: A reading comprehension benchmark requiring discrete reasoning over paragraphs. *ArXiv Preprint ArXiv:1903.00161*.

Duistermaat, J. J., & Kolk, J. A. C. (2012). *Lie groups*. Springer Science & Business Media.

Easton, R. W. (1993). Introduction to Hamiltonian dynamical systems and the N-body problem (KR Meyer and GR Hall). *SIAM Review*, *35*(4), 659.

Elsage, N., Olsson, C., Amodei, D., Olah, C., & Kaplan, J. (2022). Toy Models of Superposition. *Transformer Circuits Thread*.

Feng, Y., Chen, X., Lin, B. Y., Wang, P., Yan, J., & Ren, X. (2020). Scalable Multi-Hop Relational Reasoning for Knowledge-Aware Question Answering. *EMNLP 2020 - 2020 Conference on Empirical Methods in Natural Language Processing, Proceedings of the Conference*, 1295–1309. https://doi.org/10.18653/v1/2020.emnlp-main.99

Feynman, R. (1967). The character of physical law (1965). *Cox and Wyman Ltd., London*.

Friston, K. (2010). The free-energy principle: a unified brain theory? *Nature Reviews Neuroscience*, *11*(2), 127–138.

Fujimoto, K., & Sugie, T. (2001). Canonical transformation and stabilization of generalized Hamiltonian systems. *Systems & Control Letters*, *42*(3), 217–227. https://doi.org/10.1016/S0167-6911(00)00091-8

Garbuio, M., & Lin, N. (2021). Innovative idea generation in problem finding: Abductive reasoning, cognitive impediments, and the promise of artificial intelligence. *Journal of Product Innovation Management*, *38*(6), 701–725. https://doi.org/10.1111/JPIM.12602

Geirhos, R., Jacobsen, J. H., Michaelis, C., Zemel, R., Brendel, W., Bethge, M., & Wichmann, F. A. (2020). Shortcut learning in deep neural networks. *Nature Machine*

Intelligence 2020 2:11, *2*(11), 665–673. https://doi.org/10.1038/s42256-020-00257-z

Glattfelder, J. B. (2019). The Semantics of Symmetry, Invariance, and Structure. *Frontiers Collection, Part F1071*, 65–92. https://doi.org/10.1007/978-3-030-03633-1_3/FIGURES/1

Goldman. (1967). A causal theory of knowing. *Journal of Philosophy, 64(12)*, 357–372. https://doi.org/10.1515/9783110843828.138/HTML

Goldman, W. M. (1984). The symplectic nature of fundamental groups of surfaces. *Advances in Mathematics, 54*(2), 200–225.

Goldstein, P., & Poole, C. (2002). *Classical Mechanics*. Addison Wesley.

Hairer, E., Hochbruck, M., Iserles, A., & Lubich, C. (2006). Geometric Numerical Integration. *Oberwolfach Reports, 3*(1), 805–882. https://doi.org/10.4171/OWR/2006/14

Hélie, S., & Sun, R. (2010). Incubation, insight, and creative problem solving: a unified theory and a connectionist model. *Psychological Review, 117*(3), 994.

Hirsch, M. W., Smale, S., & Devaney, R. L. (2013). *Differential equations, dynamical systems, and an introduction to chaos*. Academic press.

Ho, X., Nguyen, A. K. D., Sugawara, S., & Aizawa, A. (2020). Constructing A Multi-hop QA Dataset for Comprehensive Evaluation of Reasoning Steps. *COLING 2020 - 28th International Conference on Computational Linguistics, Proceedings of the Conference*, 6609–6625. https://doi.org/10.18653/v1/2020.coling-main.580

Järvelä, S., Nguyen, A., & Hadwin, A. (2023). Human and artificial intelligence collaboration for socially shared regulation in learning. *British Journal of Educational Technology, 54*(5), 1057–1076. https://doi.org/10.1111/BJET.13325

Jhamtani, H., & Clark, P. (2020a). Learning to Explain: Datasets and Models for Identifying Valid Reasoning Chains in Multihop Question-Answering. *EMNLP 2020 - 2020 Conference on Empirical Methods in Natural Language Processing, Proceedings of the Conference*, 137–150. https://doi.org/10.18653/v1/2020.emnlp-main.10

Jhamtani, H., & Clark, P. (2020b). Learning to explain: Datasets and models for identifying valid reasoning chains in multihop question-answering. *ArXiv Preprint ArXiv:2010.03274*.

Jolliffe, I. T., & Cadima, J. (2016). Principal component analysis: a review and recent developments. *Philosophical Transactions of the Royal Society A: Mathematical, Physical and Engineering Sciences, 374*(2065), 20150202.

Kaelbling, L. P., Littman, M. L., & Moore, A. W. (1996). Reinforcement Learning: A Survey. *Journal of Artificial Intelligence Research, 4*, 237–285. https://doi.org/10.1613/JAIR.301

Karasev, M. V., & Maslov, V. P. (2012). *Nonlinear Poisson brackets: geometry and quantization* (Vol. 119). American Mathematical Soc.

Khot, T., Clark, P., Guerquin, M., Jansen, P., & Sabharwal, A. (2020). QASC: A Dataset for Question Answering via Sentence Composition. *Proceedings of the AAAI Conference on Artificial Intelligence, 34*(05), 8082–8090. https://doi.org/10.1609/AAAI.V34I05.6319

Kosmann-Schwarzbach, Y., Schwarzbach, B. E., & Kosmann-Schwarzbach, Y. (2011). *The noether theorems*. Springer.

Kounios, J., & Beeman, M. (2014a). The cognitive neuroscience of insight. *Annual Review of Psychology, 65*(1), 71–93.

Kounios, J., & Beeman, M. (2014b). The cognitive neuroscience of insight. *Annual Review of Psychology, 65*(1), 71–93.

Kuhn, T. S. (1962). *The structure of scientific revolutions* (Vol. 962). University of Chicago press.

Lipton, Z. C. (2018). The mythos of model interpretability: In machine learning, the concept of interpretability is both important and slippery. *Queue, 16*(3), 31–57.

Maruthi, S., Dodda, S. B., Yellu, R. R., Thuniki, P., Reddy, S., & Reddy, B. (2022). Temporal Reasoning in AI Systems: Studying temporal reasoning techniques and their applications in AI systems for modeling dynamic environments. *Journal of AI-Assisted Scientific Discovery, 2*(2), 22–28. https://scienceacadpress.com/index.php/jaasd/article/view/16

Mehrabi, N., Morstatter, F., Saxena, N., Lerman, K., & Galstyan, A. (2021). A Survey on Bias and Fairness in Machine Learning. *ACM Computing Surveys (CSUR), 54*(6). https://doi.org/10.1145/3457607

Mehta, P., Bukov, M., Wang, C. H., Day, A. G. R., Richardson, C., Fisher, C. K., & Schwab, D. J. (2019). A high-bias, low-variance introduction to Machine Learning for physicists. *Physics Reports, 810*, 1–124. https://doi.org/10.1016/j.physrep.2019.03.001

Mihaylov, T., Clark, P., Khot, T., & Sabharwal, A. (2018). Can a suit of armor conduct electricity? a new dataset for open book question answering. *ArXiv Preprint ArXiv:1809.02789*.

Mikolov, T., Sutskever, I., Chen, K., Corrado, G. S., & Dean, J. (2013a). Distributed Representations of Words and Phrases and their Compositionality. *Advances in Neural Information Processing Systems, 26*.

Mikolov, T., Sutskever, I., Chen, K., Corrado, G. S., & Dean, J. (2013b). Distributed Representations of Words and Phrases and their Compositionality. *Advances in Neural Information Processing Systems, 26*.

Olson, C. L. (1979). *Practical considerations in choosing a MANOVA test statistic: a rejoinder to Stevens*.

O'neill, B. (2006). *Elementary differential geometry*. Elsevier.

Pennington, J., Socher, R., & Manning, C. D. (2014). Glove: Global vectors for word representation. *Proceedings*

of the 2014 Conference on Empirical Methods in Natural Language Processing (EMNLP), 1532–1543.

Penrose, R. (2006). *The road to reality*. Random house.

Popper, K. (1959). *The logic of scientific discovery*. Routledge.

Prugovečki, E. (1979). Stochastic phase spaces and master Liouville spaces in statistical mechanics. *Foundations of Physics, 9*(7–8), 575–587. https://doi.org/10.1007/BF00708370/METRICS

Quine, W. V. O. (1948). *On what there is*. Catholic University of America, Philosophy Education Society Washington, DC.

Rahutomo, F., Kitasuka, T., & Aritsugi, M. (2012). Semantic cosine similarity. *The 7th International Student Conference on Advanced Science and Technology ICAST, 4*(1), 1.

Reimers, N. (2019). Sentence-BERT: Sentence Embeddings using Siamese BERT-Networks. *ArXiv Preprint ArXiv:1908.10084*.

Ribeiro, M. T., Singh, S., & Guestrin, C. (2016). "Why should i trust you?" Explaining the predictions of any classifier. *Proceedings of the ACM SIGKDD International Conference on Knowledge Discovery and Data Mining, 13-17-August-2016*, 1135–1144. https://doi.org/10.1145/2939672.2939778/SUPPL_FILE/KDD2016_RIBEIRO_ANY_CLASSIFIER_01-ACM.MP4

Rosenthal, R., Cooper, H., & Hedges, L. (1994). Parametric measures of effect size. *The Handbook of Research Synthesis, 621*(2), 231–244.

Russo, D. J., Van Roy, B., Kazerouni, A., Osband, I., & Wen, Z. (2018). A Tutorial on Thompson Sampling. *Foundations and Trends® in Machine Learning, 11*(1), 1–96. https://doi.org/10.1561/2200000070

Sennrich, R. (2015). Neural machine translation of rare words with subword units. *ArXiv Preprint ArXiv:1508.07909*.

Singh, C., Inala, J. P., Galley, M., Caruana, R., & Gao, J. (2024). *Rethinking Interpretability in the Era of Large Language Models*. https://arxiv.org/abs/2402.01761v1

Spivey, M. J., & Dale, R. (2006). Continuous dynamics in real-time cognition. *Current Directions in Psychological Science, 15*(5), 207–211.

Strogatz, S. H. (2018). *Nonlinear dynamics and chaos: with applications to physics, biology, chemistry, and engineering*. CRC press.

Sussillo, D., & Barak, O. (2013). Opening the black box: low-dimensional dynamics in high-dimensional recurrent neural networks. *Neural Computation, 25*(3), 626–649.

Tegmark, M. (2008). The mathematical universe. *Foundations of Physics, 38*(2), 101–150.

Wang, X., Liu, K., Wang, D., Wu, L., Fu, Y., & Xie, X. (2022). Multi-level Recommendation Reasoning over Knowledge Graphs with Reinforcement Learning. *WWW 2022 - Proceedings of the ACM Web Conference 2022*, 2098–2108. https://doi.org/10.1145/3485447.3512083/SUPPL_FILE/SUPPLEMENTARY.ZIP

Weinberg, S. (1995). *The quantum theory of fields* (Vol. 2). Cambridge university press.

Welbl, J., Stenetorp, P., & Riedel, S. (2018). Constructing Datasets for Multi-hop Reading Comprehension Across Documents. *Transactions of the Association for Computational Linguistics, 6*, 287–302. https://doi.org/10.1162/TACL_A_00021/43434/CONSTRUCTING-DATASETS-FOR-MULTI-HOP-READING

Wigner, E. P. (1990). The Unreasonable Effectiveness of Mathematics in the Natural Sciences. *Mathematics and Science*, 291–306. https://doi.org/10.1142/9789814503488_0018

Worrall, J. (1989). Structural Realism: The Best of Both Worlds? *Dialectica, 43*(1–2), 99–124. https://doi.org/10.1111/J.1746-8361.1989.TB00933.X

Wu, T., Fischer, I., Chuang, I. L., & Tegmark, M. (2020). Learnability for the information bottleneck. *Uncertainty in Artificial Intelligence*, 1050–1060.

Yang, Z., Qi, P., Zhang, S., Bengio, Y., Cohen, W. W., Salakhutdinov, R., & Manning, C. D. (2018a). HOTPOTQA: A Dataset for Diverse, Explainable Multi-hop Question Answering. *ArXiv Preprint*. https://wiki.sh/

Yang, Z., Qi, P., Zhang, S., Bengio, Y., Cohen, W. W., Salakhutdinov, R., & Manning, C. D. (2018b). HotpotQA: A dataset for diverse, explainable multi-hop question answering. *ArXiv Preprint ArXiv:1809.09600*.

Zabelina, D. L., & Andrews-Hanna, J. R. (2016). Dynamic network interactions supporting internally-oriented cognition. *Current Opinion in Neurobiology, 40*, 86–93.

Zhang, W. E., Sheng, Q. Z., Alhazmi, A., & Li, C. (2020). Adversarial Attacks on Deep-learning Models in Natural Language Processing. *ACM Transactions on Intelligent Systems and Technology (TIST), 11*(3). https://doi.org/10.1145/3374217